Board of Studies
in Chemistry

PROJECT REPORT

in part-fulfilment of the requirements
for the Degree of Master of Chemistry

Title   Star Polymer–Protein Conjugates to Study Movement of Proteins in Bacterial Cell Membranes

Author   Hanni Haapsaari

Date   May 2022

Contents

Abbreviations

ATRP	–	atom transfer radical polymerisation	OPAL	–	organocatalyst-mediated protein aldol ligation
DLS	–	dynamic light scattering	RAFT	–	reversible addition–fragmentation chain transfer polymerisation
DNA	–	deoxyribonucleic acid			
GPC	–	gel permeation chromatography	RNA	–	ribonucleic acid
NAG	–	*N*-acetylglucosamine	SDS-PAGE	–	sodium dodecyl sulphate polyacrylamide gel electrophoresis
NAM	–	*N*-acetylmuramic acid			
NMR	–	nuclear magnetic resonance	SET-LRP	–	single-electron transfer living radical polymerisation
Omp	–	outer membrane protein			
			WHO	–	World Health Organisation

Abstract

Antibiotic resistance in bacteria is a rapidly growing issue worldwide. Especially, a lack of efficient antibiotics against Gram-negative bacteria is a problem since they have an outer membrane that provides additional protection against defence factors. Outer membrane proteins move to the cell poles during cell division. Preventing this movement could potentially disrupt cell division and provide a new approach to antibiotic development. Star polymer–colicin conjugates might bind the proteins together and thus prevent their movement. This project aimed to produce a small library of star polymers and conjugate them to model protein myoglobin. Star polymers were successfully synthesised by single-electron transfer living radical polymerisation. Their indicative sizes were determined by dynamic light scattering, although aggregation complicated this. End-group conversions were performed to introduce required aldehyde functionality, but no definite characterisations were obtained by ^{1}H NMR because of dominant polymer peaks. However, the conversions were confirmed successful for a small linear polymer synthesised by identical methods. Organocatalyst-mediated protein aldol ligation was tried for conjugation, but gel electrophoresis staining was not sensitive enough for final confirmation. However, dynamic light scattering studies indicate bigger particles than either of the starting materials, which is promising. These results could be used to choose an optimal size of star polymers to be conjugated to colicins. How the binding of these conjugates affects outer membrane protein movement can be studied by fluorescence microscopy.

1 Introduction

Antibiotic resistance in bacteria continues to be a rapidly growing and health-endangering issue worldwide.[1] Our ability to treat common bacterial infections is threatened by the emergence and spread of antibiotic-resistant bacteria as they constantly develop new resistance mechanisms and antibiotics become less and less effective.[2] Especially, a lack of efficient antibiotics against Gram-negative bacteria[2] is a problem since they are naturally more resistant to defence factors that are very toxic to Gram-positive bacteria.[3–5] Gram-negative bacteria, such as *Klebsiella pneumoniae* and *Escherichia coli*, can cause severe and deadly infections in the urinary tract, upper respiratory tract, biliary tract, skin, soft tissues, bones, joints, and eyes, and lead to sepsis.[6] Without effective treatment, these infections threaten those with weak immune systems.[2] Medical procedures, surgeries, for instance, become riskier as well. For example, in 2020, the median resistance to ciprofloxacin, a common antibiotic against urinary tract infections, was 43.1% for *E. coli* and 36.4% for *K. pneumoniae* worldwide.[7] At the same time, in some countries, resistance to carbapenem antibiotics, which are usually last resort treatments against urinary tract infections, was detected in 15% of the patients with *E. coli* infections and over 50% of the patients with *K. pneumoniae* infections. Even more concerning is the detection of resistance against antibiotic colistin in several countries. Colistin is currently the only last resort treatment for carbapenem-resistant *Enterobacteriaceae* infections.[8] The need for new antibiotics is therefore urgent.

Currently, the clinical pipeline for new antibiotics and the amount of recently approved antibiotics are inadequate to overcome the challenges of increasing antibiotic resistance.[9] One issue is that the profit from an investment in antibiotics is less favourable compared to other drugs.[10] A study from 2017 estimates the cost of developing a new antibiotic at around US$1600 million.[11] Antibiotics are generally prescribed for a couple of weeks at a time, so their treatment cycle is short, which reduces the amount that can be sold.[12] This, in turn, makes the estimated net present value negative for an investment in a new antibiotic.[11] Developing and bringing new antibiotics to market is unprofitable, so many large pharmaceutical companies have

concentrated on more profitable lines of drug development.

The current clinical antibiotic pipeline contains 43 antibiotics, of which 26 are effective against the WHO priority pathogens like *Enterobacteriaceae*.[9] Half of these 26 antibiotics target at least one of the critical groups of Gram-negative bacteria. Only two of these have activity against all three critical priority pathogen classes: carbapenem-resistant *Enterobacteriaceae*, carbapenem-resistant *Acinetobacter baumannii*, and carbapenem-resistant *Pseudomonas aeruginosa*. In addition, of the 26 antibiotics in the clinical phase targeting WHO's priority pathogens, only seven fulfil at least one of WHO's innovation criteria: no known cross-resistance, new class, new target, or a new mode of action. The problem with antibiotics that are derivatives of existing antibiotics is that multiple resistance mechanisms already exist, and the possibility of resistance to these new antibiotics is high. Of the seven innovative antibiotics, only two are active against the critical Gram-negative bacteria. Therefore, there is a major shortage of antibiotics that are both innovative and target the critical Gram-negative bacteria. To avoid cross-resistance, new classes of antibiotics are needed with new modes of action and new targets.[13]

1.1 Bacterial outer membrane

All bacteria have an inner membrane (Figure **1c**), which is a phospholipid bilayer[14], and a cell wall (Figure **1b**) consisting of peptidoglycan.[15] This peptidoglycan layer in Gram-positive bacteria is considerably thicker than in Gram-negative bacteria, and this difference allows the Gram-negative and Gram-positive bacteria to be distinguished. Gram-staining is a method by which bacteria can be classified into these groups.[16] A primary stain is retained in a thicker peptidoglycan layer, and Gram-positive bacteria remain purple after staining. The primary stain can be washed out from a thinner layer, and the cells can instead be stained with a counterstain leaving them red. In addition to an inner membrane and a cell wall, Gram-negative bacteria have an outer membrane (Figure **1a**) which is a trilaminar structure located outside the peptidoglycan layer.[15] It is important in the function of Gram-negative bacteria, and this additional membrane

makes Gram-negative bacteria more resistant to host defence factors and antibiotics.[3–5,17] It acts as a permeability barrier consisting of lipopolysaccharides. The membrane has a hydrophilic surface because of polysaccharides bound to it which provide complementary resistance.[5,18,19] They also help evade phagocytosis and avoid specific immune system responses by altering the antigen composition on the surface.[20–22]
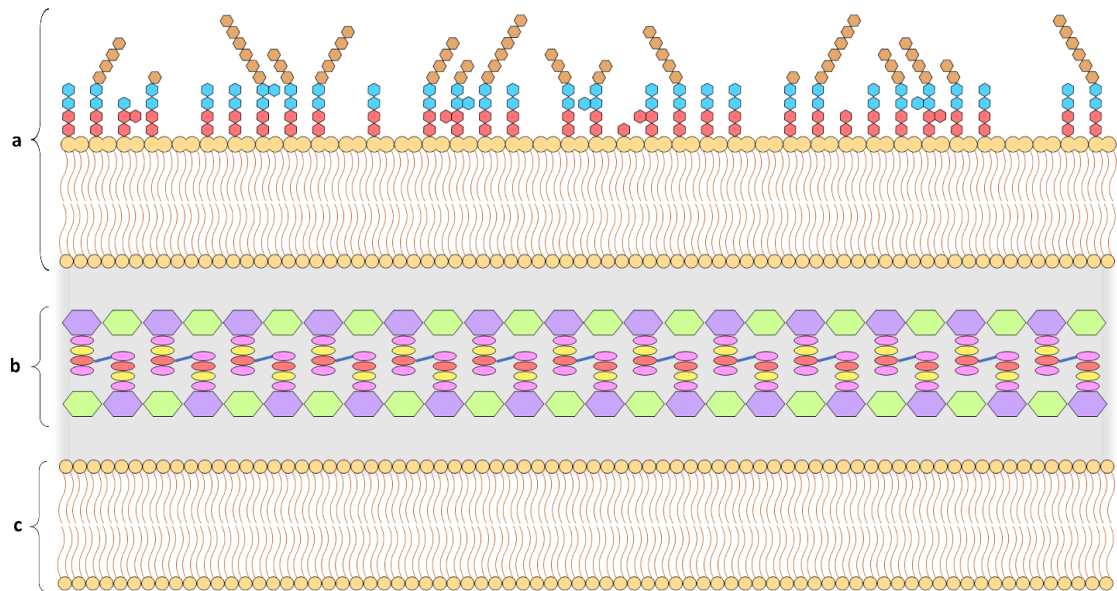

Figure 1: Typical membrane structure of Gram-negative bacteria consisting of **(a)** an outer membrane, **(b)** a cell wall, and **(c)** an inner membrane.

The inner membrane is composed of phospholipids.[15] A phospholipid has two hydrophobic fatty acids connected to a hydrophilic phosphate group via an alcohol residue (Figure **2a**). Phospholipids are amphiphilic, and aggregation of lipid chains in aqueous solutions results in a lipid bilayer with a hydrophilic surface. The peptidoglycan cell wall, in turn, comprises peptidoglycan polymers which consist of amino acids and carbohydrates (Figure **2b**). The saccharide part has alternating *N*-acetylglucosamine (NAG) and *N*-acetylmuramic acid (NAM) residues. A short, three to five amino acids long peptide chain is attached to each NAM residues. Cross-linking of these amino acids leads to a lattice structure. The trilaminar structure of the outer membrane stems from a lipid bilayer and polysaccharides bound to it. The phospholipid compositions of the inner and outer membranes are usually very similar. The other layer of the lipid bilayer is formed by lipopolysaccharides which consist of three parts: lipid A, core, and O-antigen (Figure **2c**). Lipid A is a disaccharide connected to multiple fatty acids. While phospholipids have two fatty acid chains connected to the disaccharide backbone, lipopolysaccharides have

six or seven fatty acid chains linked to the glucosamine backbone. Contrary to phospholipids, all lipopolysaccharide fatty acid chains are saturated, and some are 3-hydroxy fatty acids. These 3-hydroxy groups can connect fatty acid chains, producing characteristic 3-acyl-oxy-acyl structures. The core part is attached to the lipid A, and its structure is subdivided into an inner and an outer core, both of which are oligosaccharides. The outermost part of the lipopolysaccharide is an O-antigen attached to the core part. O-antigen is a polysaccharide, but its carbohydrate composition varies from strain to strain, leading to specific antigenicity. On entering the body, O-antigens provoke an immune response, and lipid A acts as an endotoxin and is responsible for most of the toxicity of Gram-negative bacteria.
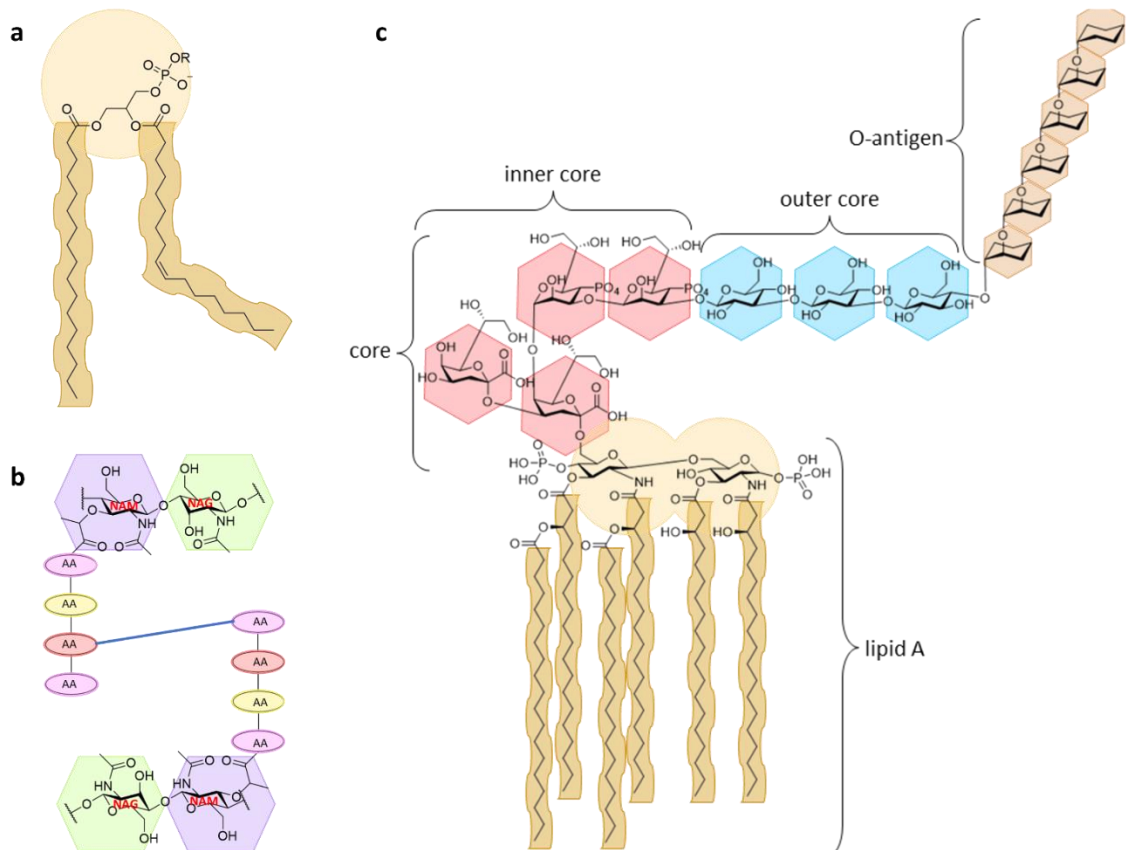

Figure 2: General structures of **(a)** a phospholipid, **(b)** peptidoglycan, and **(c)** a lipopolysaccharide.

1.1.1 Outer membrane proteins

Almost 50 % of the mass of the outer membrane is protein.[23] These proteins are embedded in the outer membrane as either lipoproteins or integral membrane proteins and are crucial to the function of the bacterial cell. Tasks that they perform include, for example, signal transduction[24] and solute or protein translocation[25]. As opposed to inner membrane proteins that consist of transmembrane α-helices, outer membrane proteins are β-barrels.[26] A few proteins are expressed in high concentrations, whereas minor proteins are generally synthesised when needed. There are six major classes of outer membrane proteins: the OmpA protein, the OmpX protein, general porins, substrate-specific porins, phospholipase A proteins, and TonB-dependent transporters.

The outer membrane protein A (OmpA) is one of the major outer membrane proteins.[27] It has two domains, one of which is anchored to the membrane and the other located in the periplasm interacting with the peptidoglycan layer. Providing this physical linkage between peptidoglycan and the outer membrane is assumed to be the function of OmpA.[28,29] Outer membrane protein X (OmpX) is important for the virulence of the bacterial cell as it neutralises host defence mechanisms.[30] General porins such as OmpF enable diffusion of hydrophilic molecules that otherwise could not cross the hydrophobic membrane.[25] General porins are not specific to any molecules, unlike substrate-specific porins whose channels have specificity for designated substrates.[31] An example of a substrate-specific porin would be maltooligosaccharide-specific porin LamB. Phospholipase A proteins are enzymes that participate in colicin release from *E. coli* by being involved in the hydrolysis of phospholipids.[32] TonB-dependent receptors contribute to the uptake of some larger molecules such as vitamin B12[33] or iron–siderophore complexes[34] into the bacterial cells.

1.1.2 Colicins and their binding to outer membrane proteins

Bacteriocins are antibiotic peptides or proteins produced by some strains of bacteria to kill competing strains, and their cytotoxic action is targeted to the species that produces them.[35] Their specificity stems from several protein–protein interactions needed for their intake into cells. Colicins are proteinaceous bacteriocins produced by some *E. coli* strains and therefore are specific for other *E. coli* strains. Understanding colicin translocation is important in providing insight into how both the inner and outer membrane can be breached to reach the cytoplasm. Over 20 different colicins have been found and identified, and they are divided into groups A and B.[36,37] Group A colicins use the Tol system for translocation across the outer membrane, and group B colicins use the Ton system (Figure **3**).
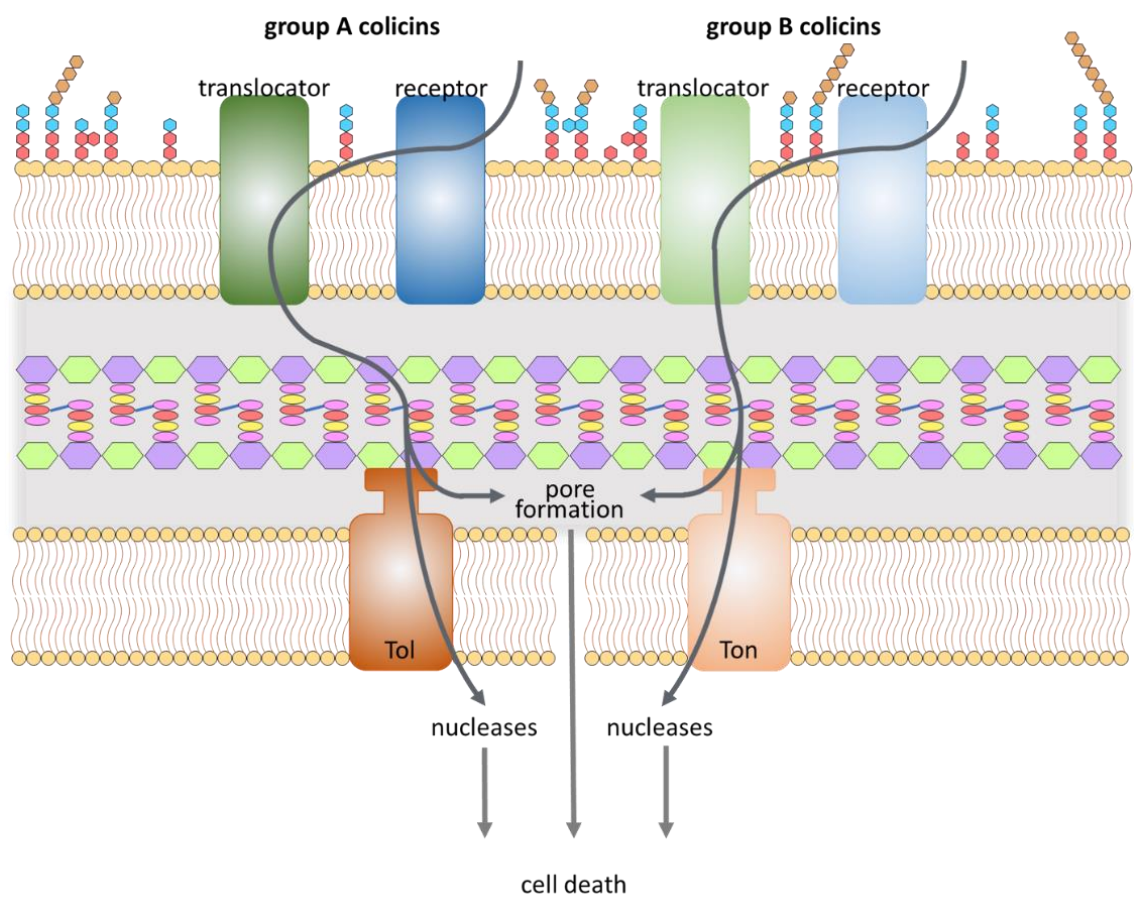

Figure 3: Colicin translocation paths into E. coli. Reproduced from reference 38.

All colicins comprise three basic modules: an amino-terminal translocation domain, a central receptor-binding domain, and a carboxy-terminal cytotoxic domain.[38] The cytotoxic domain is responsible for inducing cell death by forming a pore that depolarises the cell or cleaving DNA, transfer RNA, ribosomal RNA, or peptidoglycan. The translocation and receptor-binding domains get the cytotoxic domain across the membranes. Translocation processes for all the colicins start the same way: the receptor-binding domain binds to an outer membrane receptor with high affinity. The most common receptors that colicins bind to are β-barrels that transport vitamin B12 or iron–chelate complexes, or porins. However, colicins do not use the central channels of these receptors for translocation. Instead, they need additional proteins, translocator proteins, for translocation. An unstructured region in the translocation domain is responsible for recruiting the outer membrane translocator protein, which delivers at least one linear epitope to the periplasm. The epitopes bind to either Ton or Tol proteins, classifying colicins into groups A and B. Besides different inner membrane translocator proteins, group A and B colicins use different receptors and outer membrane translocator proteins as well. Epitope binding to Ton or Tol proteins leads to translocation of the colicin into the periplasm. If the colicin is pore-forming, it has achieved its goal because its depolarisation of the inner membrane causes cell death. Nuclease colicins need to cross the inner membrane as well to induce their cytotoxic effect.

1.2 A potential new approach to antibiotic development

Different *E. coli* strains have a wide variety of β-barrel proteins in their outer membrane.[39] As colicins bind specifically to *E. coli* outer membrane proteins, they can be used as probes to study the localisation and turnover of *E. coli* outer membrane proteins.[40] Colicins ColE9 and ColIa have been used as probes that bind to specific proteins in certain *E. coli* outer membranes. ColE9 binds to vitamin B12 transporter BtuB, and ColIa binds to an iron–siderophore transporter Cir. Disulphide bonds were introduced into the colicins to prevent translocation through the outer membrane. They were also covalently labelled with fluorophores. The localisation and turnover of outer

membrane proteins were followed by fluorescent microscopy during several cell divisions.

These studies concluded that outer membrane proteins are as clusters in the outer membrane.[40] These islands of proteins have a diameter of approximately 0.5 μm, and they consist of many different proteins. Co-localisation of different proteins and their island formation might stem from mixed protein–protein interactions. These protein islands are distributed throughout the cell. However, new outer membrane protein biogenesis was observed mainly in mid-cell during cell division. This cumulative biogenesis forces old protein islands to move to the poles of the dividing cell.

This observation could be used as a basis for new innovative antibiotics. If the movement of these protein islands was prevented, it could lead to obstruction of biogenesis of new outer membrane proteins. This, in turn, might disrupt cell division. One idea of preventing outer membrane proteins from moving in the outer membrane is to use something that binds them together. Star polymers are one option for this. Multi-arm star polymers would be conjugated to colicin proteins, which would bind to *E. coli* outer membrane proteins. The star structure would bind them together, thus preventing their movement in the outer membrane.

1.3 Star polymers

Star polymers are branched polymers where multiple linear polymer chains are linked to a central core.[41] The core can be a small molecule, a macromolecular structure, or an atom. Star polymers have smaller segment densities than their linear counterparts, which results in more compact structures.[42–44] This has an impact on many of their properties. Generally, star polymers have smaller hydrodynamic radii and internal viscosities than their linear analogues with the same molecular weight. Another one of their intriguing properties is the potential to self-assemble.[45] Aggregation into organised structures such as micelles offers many promising potential applications for star polymers, such as drug delivery. So far, star polymers have been utilised commercially

as viscosity index improvers[46] and thermoplastic elastomers[47].

A regular star polymer has homopolymer arms, but several types of different star polymers can be synthesised (Figure **4**).[48] Star polymers having block copolymer arms means that all the polymer chains are identical, but each arm is a block copolymer. Functionalised star polymers have functional groups at the end of each arm or along the arms. Asymmetric star polymers include polymers that have molecular weight, functional group, or topological asymmetry among the arms. In the case of molecular weight asymmetry, the arms have different molecular weights, but they are chemically identical. Asymmetry in functional groups means that the arms are otherwise identical, but they bear different functional groups. Topological asymmetry covers star block copolymers of which arms consist of the same copolymers, but the order of the blocks is not the same in all the arms. Miktoarms are star polymers containing chemically different arms.

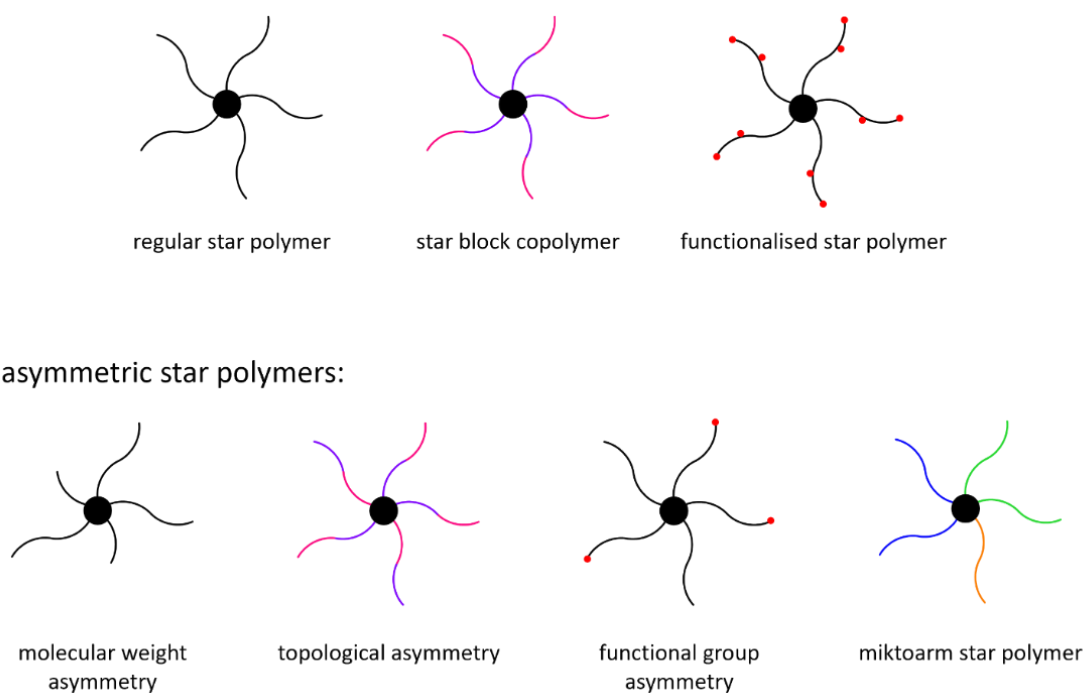| regular star polymer | star block copolymer | functionalised star polymer |

asymmetric star polymers:

| molecular weight asymmetry | topological asymmetry | functional group asymmetry | miktoarm star polymer |

Figure 4: Different star polymers.

1.3.1 Synthesis of star polymers

Three general approaches have been developed for star polymer synthesis (Figure **5**).[48] The first one is a core-first approach, where multifunctional initiators are used, and the initiator can simultaneously initiate the polymerisation of several arms. The second one is an arm-first approach that uses a cross-linker. Polymer arms are synthesised first, and then a multifunctional compound cross-links linear polymers together. The third one is a coupling-onto approach which also utilises a multifunctional core, but this time the polymer chains are synthesised first and then attached to the core.
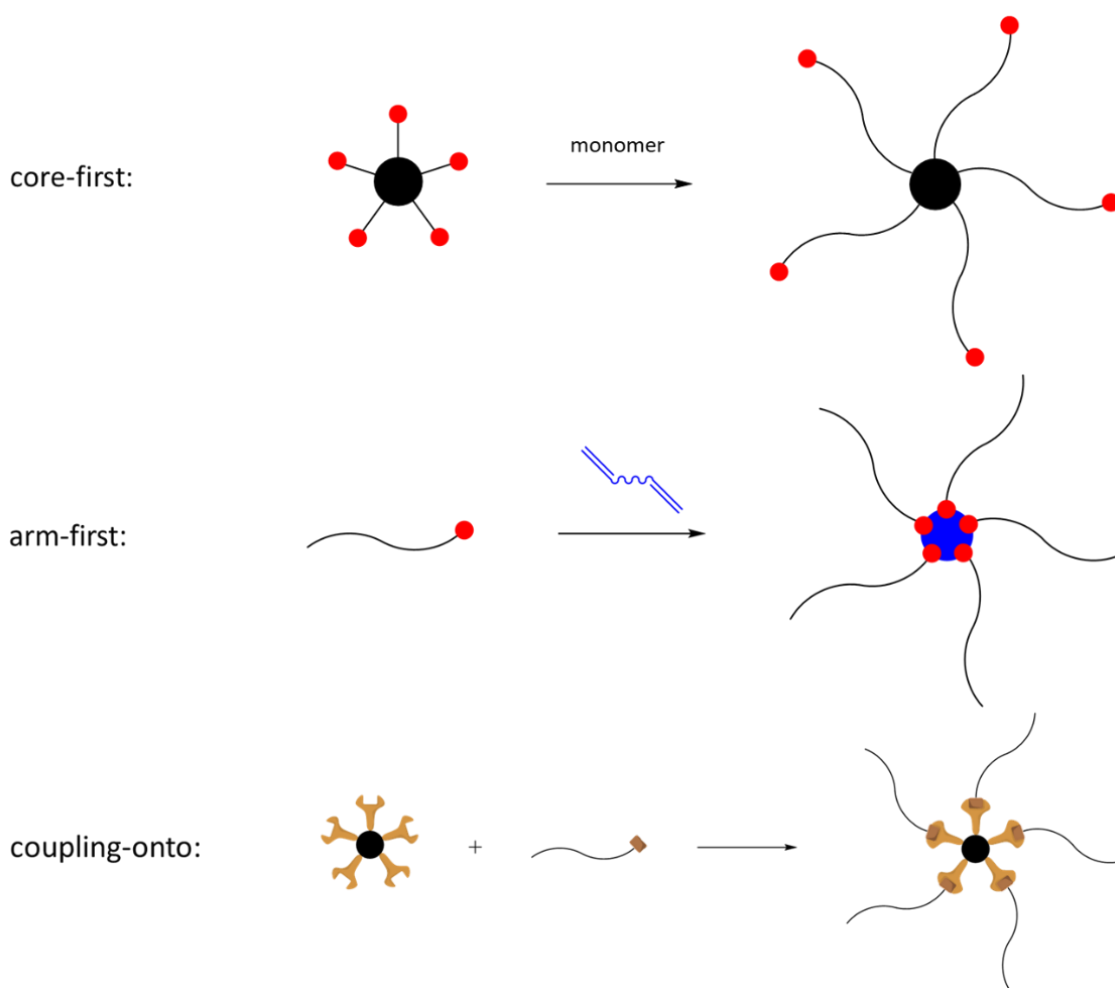

Figure 5: Three general approaches for synthesis of star polymers.

There are several synthetic strategies by which star polymers have been successfully synthesised. These include, for example, anionic polymerisation[49], cationic polymerisation[50], nitroxide-mediated polymerisation[51], atom transfer radical polymerisation (ATRP)[52], reversible addition–fragmentation chain transfer polymerisation (RAFT)[53], single-electron transfer living radical polymerisation (SET-LRP)[54], ring-opening polymerisation[55], group transfer polymerisation[56], ring-opening metathesis polymerisation[57], metal template-assisted synthesis[58], and combinations of different polymerisation techniques[59]. A good approach for star polymer synthesis is living polymerisation, which is a type of chain-growth polymerisation. Chain-growth polymerisation typically involves four reactions: initiation, chain propagation, chain termination, and chain transfer.[60] In living polymerisation, however, a possibility for the two latter reactions to occur has been removed, and therefore premature termination of polymerisation has been eliminated. Another characteristic of living polymerisation is that the rate of propagation reaction is much slower than the rate of initiation reaction, which is why all the chains grow at the rate of propagation. This means that all chains grow at the same rate, leading to polymer chains of very similar lengths and low dispersity.

1.3.2 SET-LRP

Single-electron transfer living radical polymerisation is a metal-catalysed polymerisation by which polymers with extremely high molecular weights can be generated fast.[61] The reaction occurs under mild reaction conditions at room temperature.

Scheme 1: Catalytic cycle of SET-LRP reaction. Reproduced from reference 61.

The first polymerisation step is mediated by a single-electron transfer from an electron-donating Cu(0) catalyst[61] (**a**) for it to gain a stable electronic configuration[62]. Halogen-containing initiator (**b**) acts as the electron acceptor.[61] This produces a radical-anion intermediate (**c**) and a Cu(I) species. Any polar solvent, such as DMSO decreases the interaction between the halogen anion and the electrophilic radical.[63] Proximity of the Cu(I)$^+$/L counter-cation (**d**) further facilitates the decomposition of the radical-anion pair (**c**).[61] Propagation of the polymer chain can then occur via radical addition (**f**). The generated Cu(I) species I is immediately disproportionated into Cu(0) (**a**) and Cu(II) (**g**) species. Cu(I)X spontaneously disproportionates into Cu(0) and Cu(II)X_2 species in, for example, polar solvents such as water and DMSO. This requires the presence of chelating N-containing compounds. Me$_6$TREN is the most effective ligand in DMSO. The produced Cu(II)X_2 species (**g**) then mediates the reversible termination by transferring a halide anion X$^-$ from the Cu(II) species to the propagating radical. A single-electron transfer reaction then turns the radical anion (**h**) into alkyl halide species (**b**). Continuously produced Cu(0) species then again catalyses the reactivation of these dormant alkyl halides.

SET-LRP can be applied to monomers with electron-withdrawing functional groups, like

acrylates.[61] The reaction occurs at room temperature, and only a very small amount of catalyst is needed. A low activation energy single-electron transfer process together with disproportionation of the Cu(I) species make an ultrafast living radical polymerisation possible.

1.4 Protein conjugation: OPAL chemistry

Protein–small molecule bioconjugates are becoming increasingly important and utilised in chemical biology, cell biology, and chemical medicine.[64–67] It is important to be able to conjugate small molecules to proteins with carbon–carbon bonds because they are stable in large range of conditions. Another critical requirement is that the reaction proceeds under biocompatible conditions in water and at neutral pH. Correct protein folding and functioning are dependent on the pH, and deviations from this pH may have detrimental effects on proteins and protein complexes that prevent their use in actual biological or medical applications. Organocatalyst-mediated protein aldol ligation (OPAL) enables an efficient carbon–carbon bioconjugation of small molecules to proteins at neutral pH.[68] Additional benefits of the method are affordable and simple probes and a possibility for dual modification of the OPAL product due to a β-hydroxy functionality.
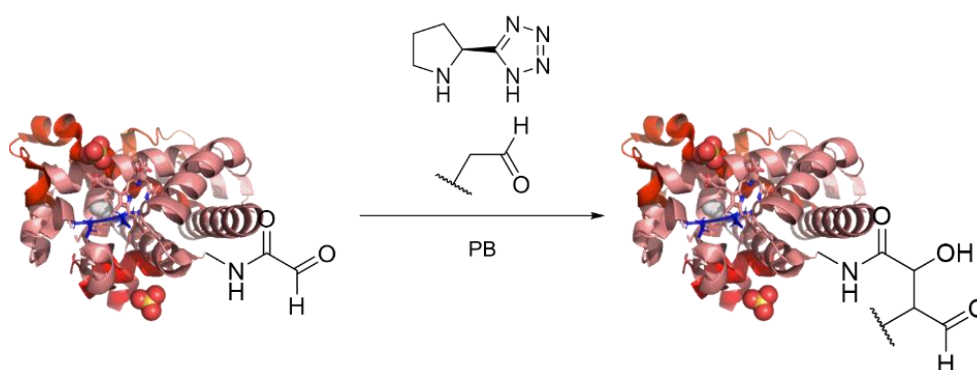
Scheme 2: A general OPAL reaction.

The α-carbon substituent of the aldehyde donor has a significant effect on the reaction rate: aldehydes with α-aryl substituents react faster than aldehydes with α-alkyl substituents.[68] The nature of the organocatalyst affects the reaction rate as well, and

tetrazole is the most efficient catalyst. First, an aldehyde donor reacts with an organocatalyst, forming an enamine-type intermediate. This intermediate then reacts with the α-oxo-aldehyde modified protein to form the small molecule–protein conjugate. The α-oxo functionality of the protein corresponds to the β-hydroxy functionality in the OPAL product. This functionality enables a dual modification by an organocatalyst-mediated β-hydroxy-oxime ligation.

OPAL reaction uses aldehydes as chemical handles that can easily be installed into both natural and unnatural proteins.[68] It combines small molecule aldehyde organocatalysis methods with bioconjugation chemistry techniques. OPAL enables site-selective ligation of proteins to aldehydes via the formation of stable carbon–carbon bonds. The reaction occurs at neutral pH at both internal and terminal sites of proteins.

1.5 Project aims and objectives

The aim of this project is to synthesise a small library of star polymers using sucrose as the core and determine degrees of polymerisation by ^{1}H NMR spectroscopy. Their dispersities will be investigated by gel permeation chromatography and their hydrodynamic diameters by dynamic light scattering. The particle size can be optimised by adjusting the degree of polymerisation. The end group linker will be attached to the chain termini and converted into an aldehyde functionality. As a model protein, myoglobin will be oxidised into glyoxyl-myoglobin to introduce a required α-oxo-aldehyde functionality. An organocatalyst-mediated protein aldol ligation (OPAL) reaction will then be performed between star polymer and glyoxyl-myoglobin to make star polymer–protein conjugates. These studies can later be used to choose an optimal degree of polymerisation and, therefore, size for star polymers, to which α-oxo-aldehyde functionalised colicin proteins would be attached. These conjugates can then be labelled with fluorophores. Their binding to *E. coli* outer membrane proteins and subsequent effect on the movement of these outer membrane proteins can be studied by fluorescent microscopy. What would be investigated is whether the binding of star polymers–colicin conjugates would prevent the movement of outer membrane protein

islands to the poles of the cells and if this disrupts new biogenesis and thus cell division. In that case, star polymer–colicin proteins could offer a potential new approach to antibiotic development that could help meet the rapidly growing issue of antibiotic-resistant bacteria.
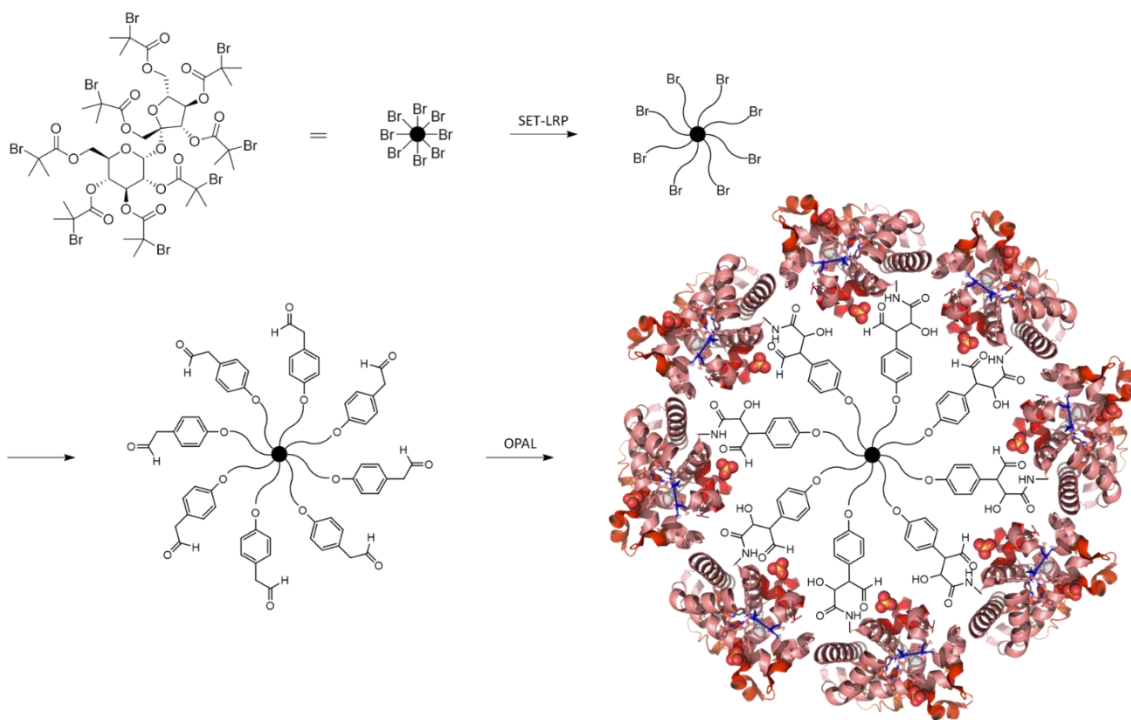

Scheme 3: The project outline.

2 Results and discussion

2.1 Sucrose-based initiator

A sucrose-based initiator **1** was synthesised to be used as a core for star polymers. Sucrose enables the creation of 8-armed star polymers, as the initiator produced from it has eight initialisation points from which a polymer chain can be grown. Sucrose is the only carbohydrate used for star polymer synthesis in this project. Glucose was another option, and it would have provided 5-armed star polymers. Based on previous studies, 8-armed star polymers are bigger than 5-armed star polymers due to the increased number of polymer arms.[69] As this project aimed to synthesise as big star polymers as possible, sucrose was chosen over glucose.
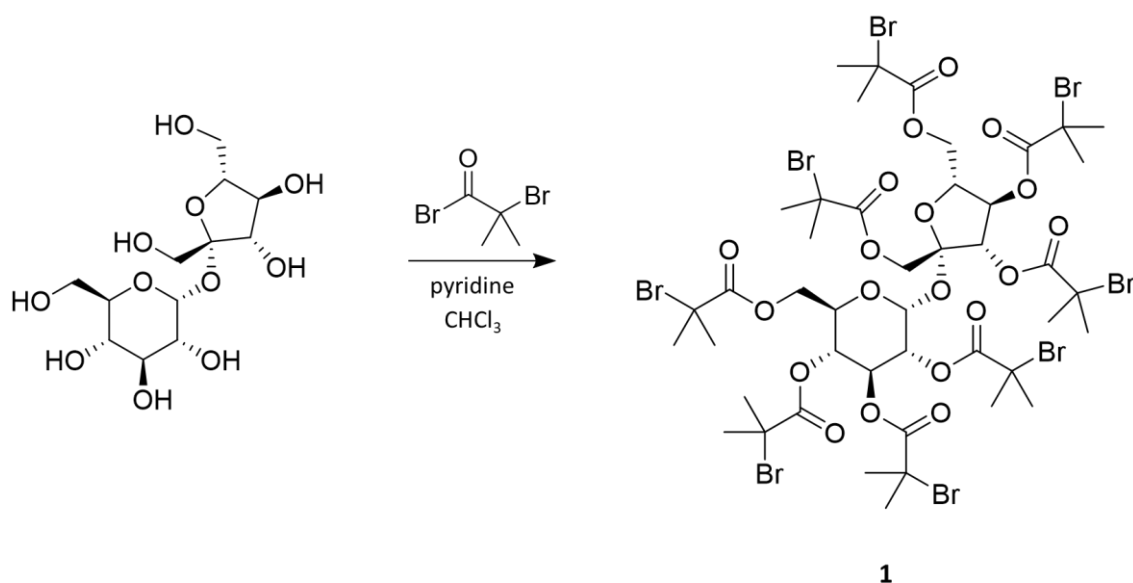
Scheme 4: Synthesis of sucrose-based initiator octakis-O-(2-bromoisobutyryl)sucrose (**1**)

Initiator **1** was synthesised using a method from the literature.[70] The first attempt at the reaction was not successful, and the reason is probably that the solvents were not as dry as they were supposed to be. New solvents were ordered, and the reaction proceeded without problems. Hence, the solvents must be anhydrous for the reaction to occur. The crude product was purified by washing with water, aqueous NaOH and

brine, and recrystallisation from methanol. Recrystallisation proved to be more challenging than anticipated. The solvent used for this was methanol, as it was used previously by other students for the same synthesis.[69,71] Some of the product always remained in methanol. This residue was then evaporated *in vacuo* and recrystallised again. In addition, the product was expected to be white. However, the product remained slightly yellow after several recrystallisations. NMR spectra showed no impurities in the slightly yellow product, but previous studies suspected that the yellow colour indicates an impurity that would prevent the following polymerisation reactions from happening[71]. A total of 6 recrystallisations were needed to get a white product. Later it was noticed that in the original publication, they reported using a mixture of methanol/H_2O (3:1) for the recrystallisations, so perhaps that solvent system would have been better and worth trying in the future, seeing as the recrystallisations were so challenging. Product **1** was characterised by ^1H NMR and ^{13}C NMR spectroscopy, mass spectrometry, and melting point.

2.2 End group linker

An end group linker **3** was synthesised as it is needed for introducing an aldehyde functionality into the polymers. An aldehyde functionality is necessary for OPAL reactions as the organocatalyst first reacts with the aldehyde in the polymers.[68] The intermediate formed by them then reacts with an α-oxo-aldehyde functionalised protein. A tyrosinol-based end group linker was synthesised by first *tert*-butyloxycarbonyl protection and then acetal protection. After attaching the linker to polymers, following deprotection and oxidation provides an aldehyde functionality in equilibrium with its hydrate from.
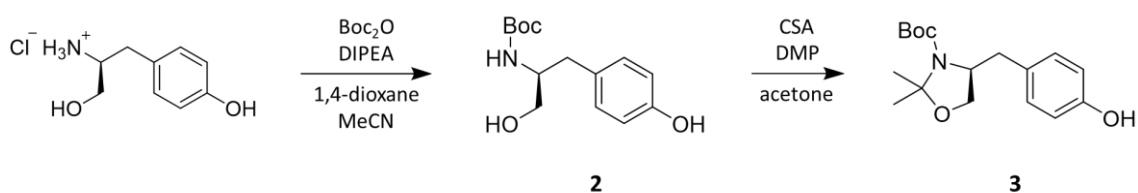

Scheme 5: Synthesis of end group linker (*S*)-*tert*-butyl-4-(4-hydroxybenzyl)-2,2-dimethyl-oxazolidine-3-carboxylate (**3**)

The end group linker **3** was synthesised using a two-step method from the literature.[68] At the first step, some problems were encountered. According to the literature method, L-tyrosinol hydrochloride is suspended in 1,4-dioxane, and aqueous NaOH solution is added. The di-*tert*-butyl dicarbonate is added to the reaction mixture. However, for some reason, the reaction did not proceed when replicating this procedure. This was suspected to be because the water in the aqueous base solution might have reacted with Boc_2O even though the reaction had worked in these conditions before. A different solvent system was thus tried. Instead of an aqueous NaOH solution, DIPEA was used as the base. However, with the original method, the starting material L-tyrosinol hydrochloride only dissolves after the addition of base because it is soluble in water. By removing water from the solvent system, another solvent was required to dissolve L-tyrosinol hydrochloride. The addition of acetonitrile was found to cause the dissolution of the starting material, after which the reaction was carried on as in the literature without further problems. The second step of the synthesis is very water-sensitive as acetal protection produces water molecules that can cause the immediate removal of the newly attached protection. To prevent this protection–deprotection equilibrium, dimethoxypropane was used as a water scavenger. This second step did not pose any problems. Both products were purified by silica gel column chromatography. Products **2** and **3** were characterised by ^1H NMR and ^{13}C NMR spectroscopy, mass spectrometry, thin layer chromatography R_f values, and melting points.

2.3 Linear polymer

Linear polymers were synthesised to test and practice SET-LRP reaction before using it to synthesise star polymers. They were also used to test end group conversions before performing the same reactions on star polymers.

2.3.1 Synthesis and characterisation
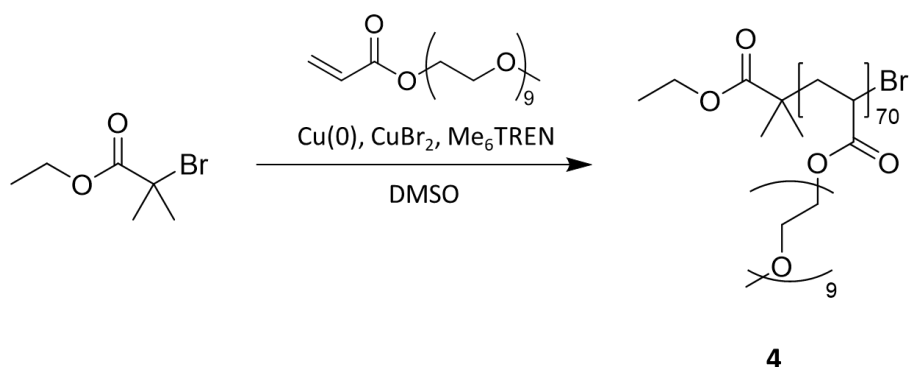
Scheme 6: Synthesis of the linear polymer **4**.

A linear polymer **4** was synthesised using SET-LRP reaction. NMR conversion analysis was used to follow the reaction. The reaction is very sensitive to oxygen as it can react with the propagating radicals and thus inhibit the polymerisation. For this reason, the reaction mixture has to be deoxygenated by sparging with argon before starting the reaction. Initially, a sparging time of 5 minutes was used, but the reaction did not proceed. The sparging time was increased to 30 minutes, after which the reaction proceeded well, and no further problems were encountered. NMR conversion analysis indicated a degree of polymerisation of 70. The crude polymer was purified by precipitation and dialysis. The linear polymer **4** was characterised by ^{1}H NMR and ^{13}C NMR spectroscopy, and GPC.

NMR conversion analysis

^{1}H NMR spectroscopy was used for conversion analysis to indicate monomer conversion. A small amount of a reference solvent was added to the reaction mixture. This solvent used was DMF, and it does not participate in the actual reaction, so it can be used as a reference. The NMR peaks that were followed were the vinyl proton peaks of the PEG acrylate monomer. The integral of these vinyl proton peaks decreases as the reaction progresses because the vinyl group is what reacts, and these protons are not present in the final product. The decrease in these integrals is directly proportional to the

monomer conversion percentage (equation **1**). The decrease can be found by comparing the integrals to the DMF reference peak integral, which stays constant throughout the reaction (Figure **9**).

$$conversion\ \% = 1 - \frac{I_t}{I_0} \times 100\% \qquad\qquad (1)$$

I_0 = the integral of the peak before starting the reaction
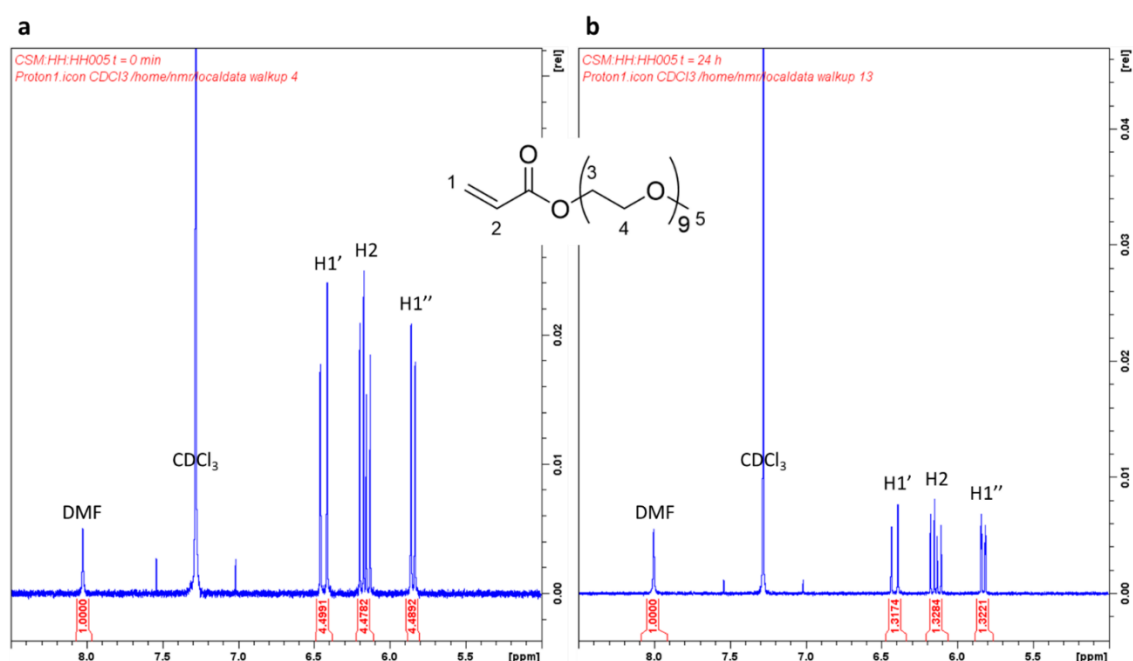
I_t = the integral of the peak after reaction time t

Figure 6: NMR conversion analysis of the linear polymer **4**. **(a)** 1H NMR spectrum of the reaction mixture at the beginning of the reaction (400 MHz, CDCl3). **(b)** 1H NMR spectrum of the reaction mixture after 24 h (400 MHz, CDCl3).

Gel Permeation Chromatography (GPC)

Gel permeation chromatography is size exclusion chromatography in which the particles are separated in a column based on their sizes. The column has porous beads inside. Bigger particles do not fit inside the pores, so they come through the column first. Smaller particles travel through the beads, and therefore their retention time is longer. Even though the separation is based on size and not molecular weight, GPC can be used to estimate the molecular weights of polymers using the calibration of standards with

known molecular weights. Number-average and weight-average molecular weights can then be used to determine the dispersity of polymers by equation **2**.

$$Đ = \frac{M_w}{M_n}$$ **(2)**

M_w = weight-average molecular weight

M_n = number-average molecular weight

In this project, GPC was used to indicate the uniformity of the linear polymer. The molecular weights obtained for the linear polymer **4** from a GPC measurement were M_n = 24 700 g mol^{-1} and M_w = 33 500 g mol^{-1} (calculated molecular weight is M = 34 000 g mol^{-1} based on ^{1}H NMR conversion analysis), and the dispersity calculated from these is Đ = 1.36. The dispersity is relatively good but not as good as expected for a SET-LRP reaction of a linear polymer. This might be due to actual inconsistencies during the reaction, although it has to be noted that the calibration and hence the obtained values most likely are not entirely reliable. The calibration is made with linear polymers, whereas the linear polymer synthesised in this project is comb-like with a potentially different coiling behaviour. So, it is possible that the measurement result is not entirely comparable to the calibration curve, and consequently, the obtained molecular weights and the dispersity value might be distorted.
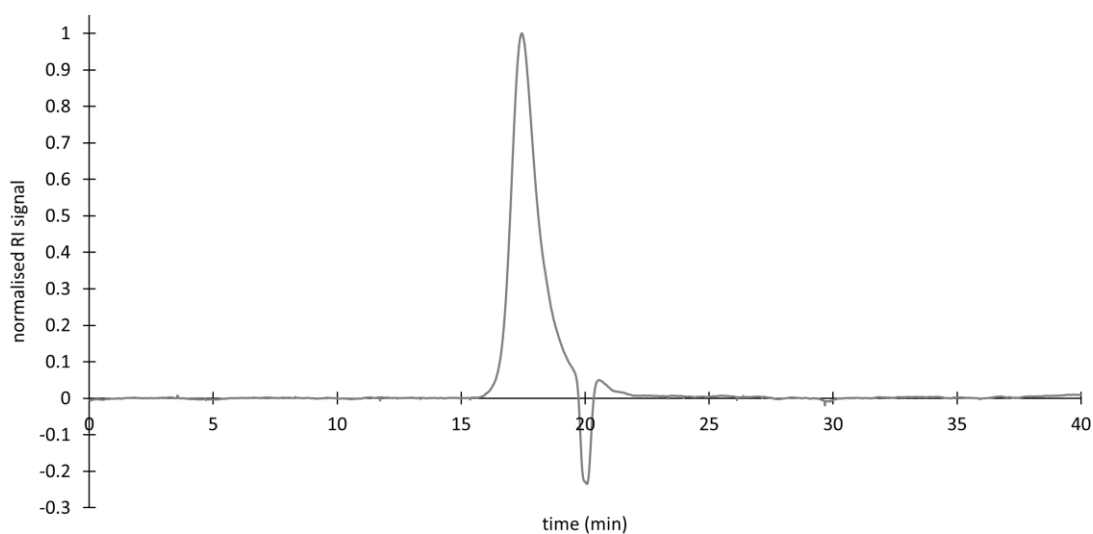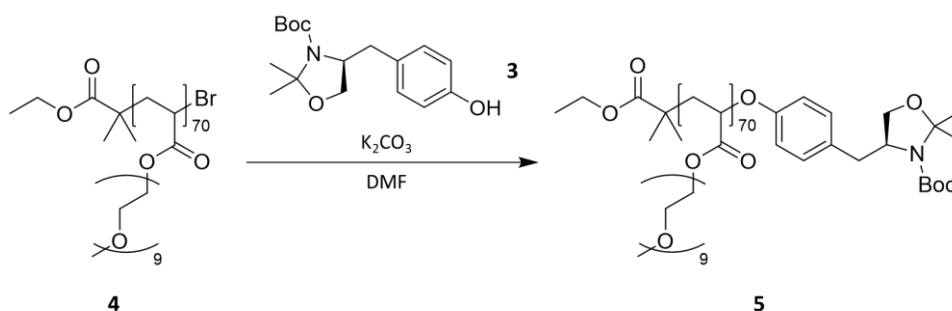

Figure 7: GPC spectrum of the linear polymer **4**.

2.3.2 End group conversions

Scheme 7: End group linker attachment to the linear polymer **4**.

The end group linker **3** was attached to the linear polymer **4** using a method used by a previous student.[71] The first attempt at the reaction was made by just dissolving all the reagents in DMF. However, nothing indicated that the reaction had occurred, so it was assumed that starting material **3** had not deprotonated. Next, the reaction was tried so that first only starting material **3** and K_2CO_3 were dissolved in DMF and heated for a few hours to ensure deprotonation. Product **4** was then added, and the reaction mixture was stirred for 48 hours. Product **5** was characterised by ^1H NMR spectroscopy. End group linker attachment was confirmed to have been successful as the NMR spectrum shows peaks in the aromatic region corresponding to the benzene ring of the end group linker (Figure 11). The integrals of these peaks are approximately 0.8, so the conversion is about 80 %.
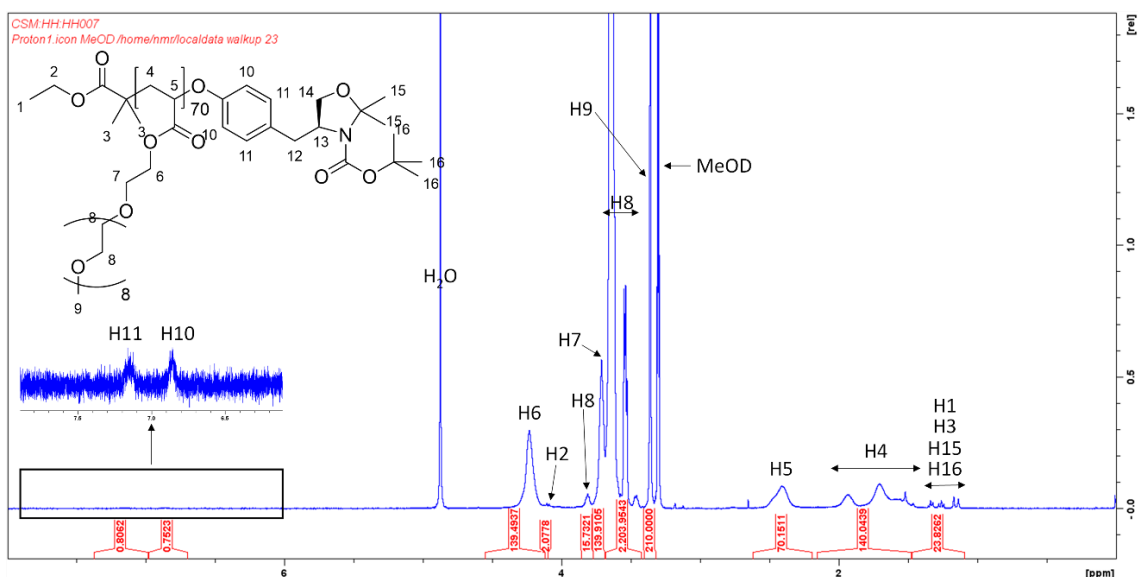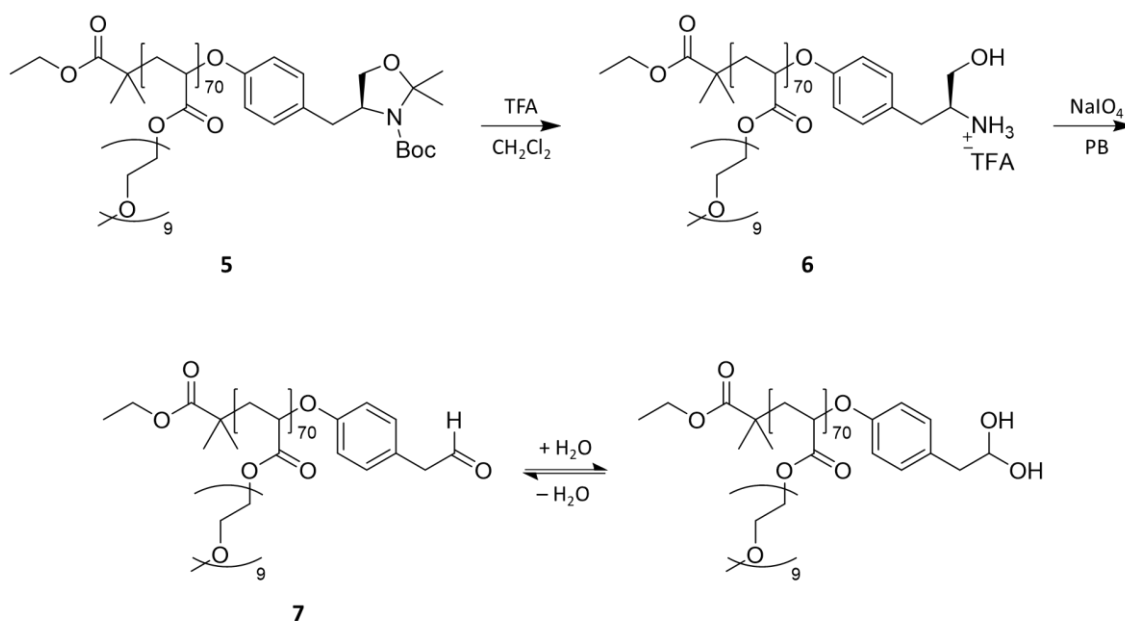

Figure 8: 1H NMR spectrum of product **5** (400 MHz, MeOD).

Scheme 8: End group modifications of product **5**.

End group modifications of product **5** were performed to get the end group linker to the desired aldehyde form. The first step is the removal of the protecting groups. Both are acid labile, so both deprotections were achieved with one step. The second step is oxidation, which produces the aldehyde functionality needed for the OPAL reactions. No apparent problems emerged during the syntheses. The only problem was the characterisation of the products. In theory, after the deprotections, there should be changes in the NMR spectra at the ≈ 1 ppm region since some of the peaks corresponding to the methyl groups of both the protecting groups should have disappeared. In practice, there are indeed some changes at the 0.7–1.3 ppm region. However, it can not be exactly identified which peaks correspond to which methyl groups due to prominent polymer peaks partly in the same area.

No definitive characterisation was obtained for product **6**, so the following oxidation reaction was started anyway in hopes that the product would offer clarity to the NMR spectra. The ^{1}H NMR spectrum of product **7** was hoped to show either a peak corresponding to the aldehyde proton or the hydrate hydroxyl protons. There is indeed a peak at 9.8 ppm, which could correspond to the aldehyde proton (Figure **12**). The integral of that is 0.3 instead of one, which is expected as most of the product should probably be in the hydrate form. Unfortunately, no hydrate protons were observed.

However, no previous NMR spectra have had a peak anywhere near 9.8 ppm, so it must be from the aldehyde proton. Based on this, it was concluded that the end group conversions were successful.
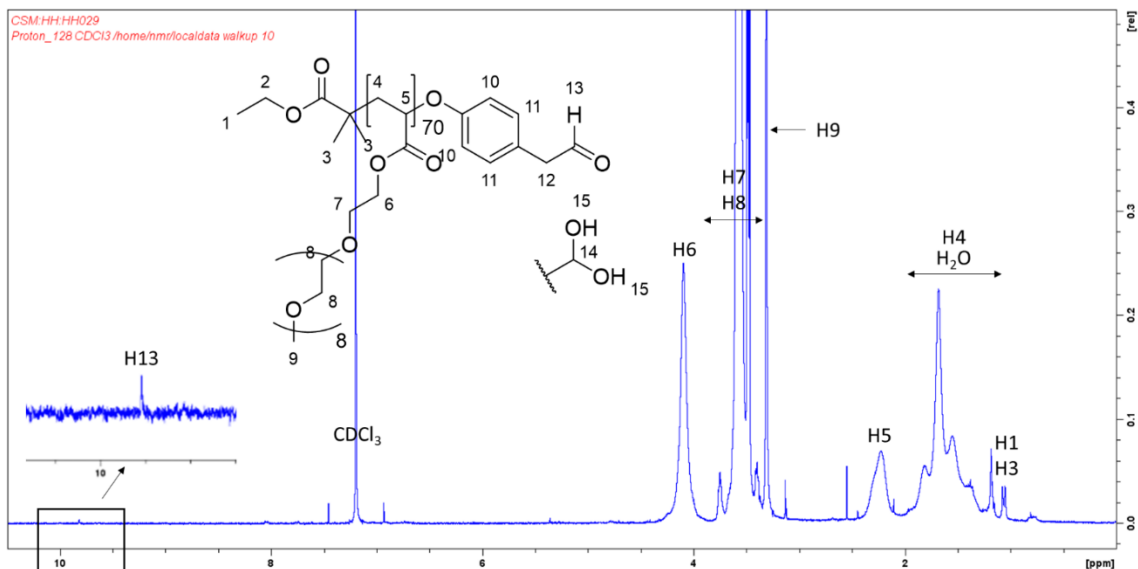

**Figure 9:** 1H NMR spectrum of product **7** (400 MHz, CDCl3).

2.4 Star polymers

A small library of star polymers was synthesised (Table **1**). Some smaller species were synthesised as well, even though the aim was to produce as big star polymers as possible.

Table 1: Star polymers synthesised in this project.

polymer	amount of monomer used (eq per arm)	monomer conversion per arm	degree of polymerisation per arm (n)	molecular weight (g mol^{-1})
8a	700	62%	430	1 700 000
8b	1250	58%	725	2 800 000
8c	2000	54%	1090	4 200 000
8d	2600	46%	1190	4 600 000
8e	3000	43%	1240	4 800 000
8f	3000	60%	1790	6 900 000
8g	5000	48%	2410	9 300 000

2.4.1 Synthesis and characterisation
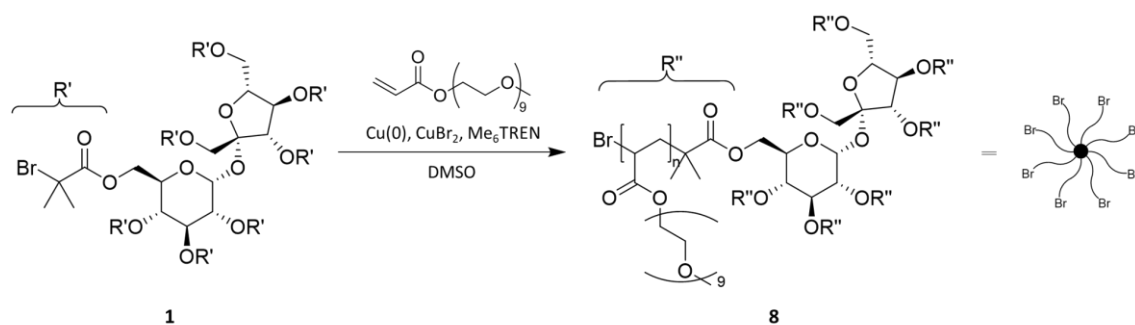
Scheme 9: Synthesis of star polymers **8a–8g**.

Star polymers were synthesised using SET-LRP reaction. The reaction execution was the same as with the linear polymer except for a different initiator (compound **1**). Conversion percentages for all the reactions were obtained from NMR conversion analyses. The syntheses were started with 2000 equivalents of monomer per initiator arm. This yielded in a product **8c** with 54 % conversion. The reaction mixture ended up being relatively viscous, which unfortunately might have affected the uniformity of the produced star polymers as reactions are slower in viscous reaction media. For the next reaction **8d**, 2600 equivalents of the monomer per arm were used, but the amounts of all the other reagents were $\frac{1}{2}$ of the amounts used for the previous reaction, which was hoped to result in a less viscous reaction mixture as the volume of the solvent was not changed. The reaction mixture was considerably less viscous by the end of the reaction, but the conversion percentage was only 46. The reason might be that perhaps not enough of the copper catalyst or the ligand was present. This would again lead to less uniform products. 0.2 equivalents per arm of both $Cu(II)Br_2$ and Me_6TREN were used for this reaction. The next reaction **8e** was started with 3000 equivalents of monomer, and the amounts of $Cu(II)Br_2$ and Me_6TREN were increased to 0.5 and 1 equivalents per arm, respectively. The amount of initiator was increased to $\frac{4}{3}$ compared to the previous reaction because the last reaction mixture was not viscous. Unfortunately, this increase, together with a bigger monomer amount, led to a highly viscous reaction mixture where the stirrer bar had stopped stirring altogether. This will have stopped the reaction, which is why the conversion percentage is even lower. In addition, this would probably have resulted in very heterogeneous polymer arm lengths. The reaction was tried again (**8f**)

with the same equivalents of monomer, Cu(II)Br$_2$, and Me$_6$TREN, but this time the amount of initiator was reduced to $\frac{1}{2}$ compared to the previous attempt. This proved effective as the conversion was 60 %, although the reaction mixture was still slightly viscous. For the final reaction **8g**, the monomer amount was increased a lot at once, and therefore the initiator amount was decreased again. However, the decrease was not enough as the reaction mixture still ended up being quite viscous. Even though the conversion percentage remained relatively low, a star polymer with much longer polymer chains was still obtained. In addition to all these, two smaller species **8a** and **8b** of star polymers were synthesised. These reactions were quenched when NMR conversion analysis indicated the desired conversion percentage. All the star polymers were characterised by ^{1}H NMR, GPC, and DLS.

Gel Permeation Chromatography (GPC)

GPC measurements were performed in hopes of obtaining dispersity values so they would provide information on star polymer homogeneity. Unfortunately, all polymers exceeded the column calibration limits, so this information was not attainable. The molecular weights and dispersities would not have been that reliable anyway because the calibration is made with linear polymers and not with star polymers or even comb-like polymers, but somewhat indicative information was hoped to be obtained. However, seeing as the polymers are too big, the only useful information from these measurements is the shapes of the peaks in the measurement graphs.

As expected, the two smaller polymers **8a** and **8b** produce the narrowest peaks, which would indicate quite good dispersity. Then again, the products **8c**, **8e**, and **8g** of the most viscous reaction mixtures produced the broadest peaks, which is not surprising as the viscosity has affected the homogeneity of the growth of the polymer arms. The peaks of the two remaining polymers **8d** and **8f** are not as broad but probably not as narrow as would be ideal either. The viscosity of the reaction mixtures is a problem as it increases the heterogeneity of the products. Even though the star polymers synthesised here are not as uniform as was hoped because of the viscosity, the project was continued with

these polymers. In the future, however, it would probably be worth it to try the syntheses in considerably bigger volumes of solvent or smaller overall amounts of reagents.
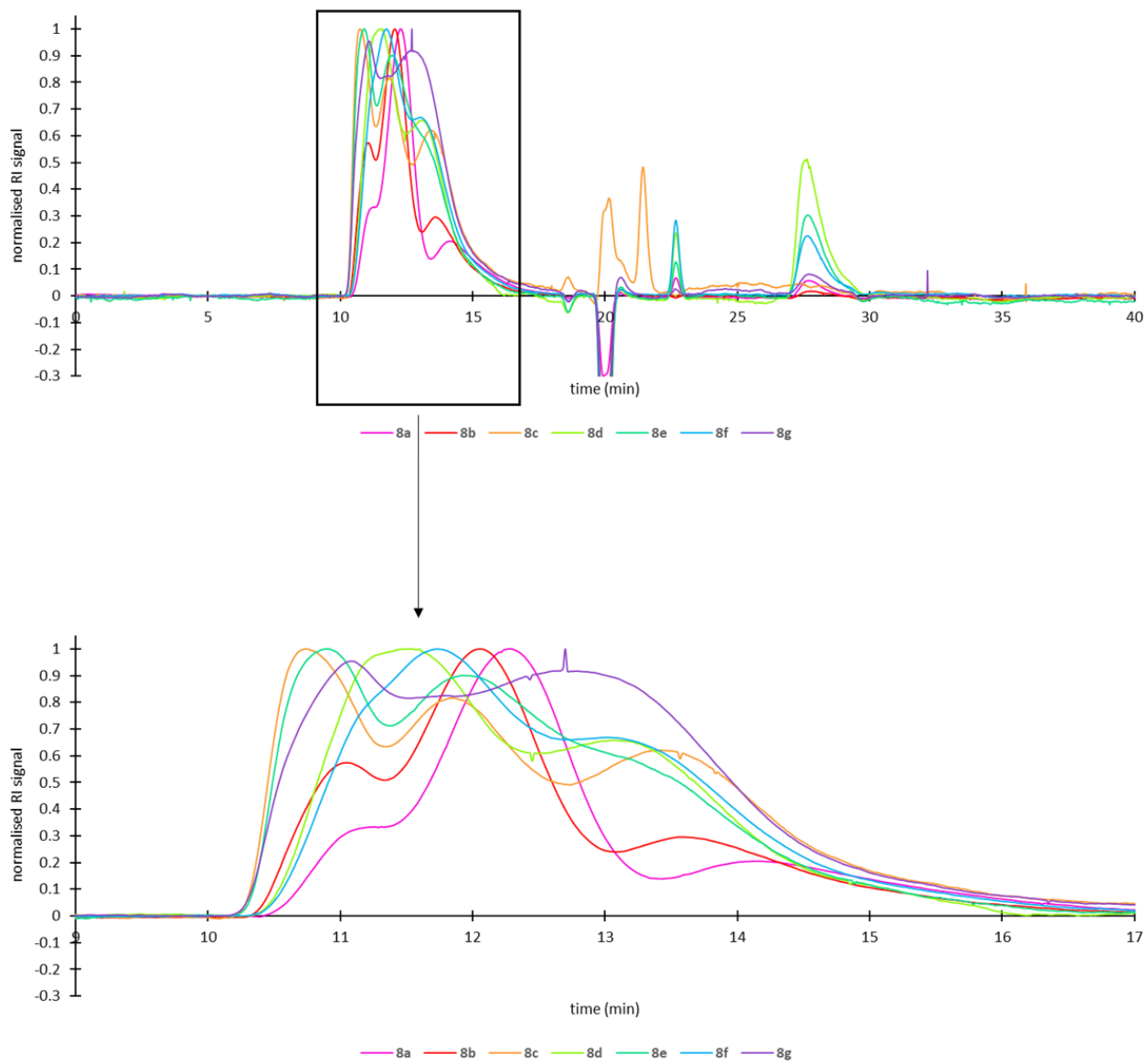

Figure 10: GPC spectra of star polymers **8a–8g**.

Dynamic Light Scattering (DLS)

Dynamic light scattering is a technique with which hydrodynamic diameters of macromolecules can be determined. DLS measurements were performed to obtain information of the hydrodynamic diameters of the star polymers. DLS utilises the Brownian motion of particles as the speed of this random motion is proportional to the size of the particles. The hydrodynamic diameters are obtained by measuring the light scattered from the macromolecules. DLS is extremely biased towards larger species of particles such as aggregates. This stems from the Rayleigh scattering theory, which says that the intensity of scattered light is proportional to the particle radius to the power of six. This means that if a particle is ten times bigger than another particle, it will produce 10^6 times bigger intensity if their quantities in the solution are the same.

Additionally, the solvent can affect the results. Solvents with higher ionic strength will lead to smaller particle sizes since the ions in the solvent reduce the length of how far a particle's electrostatic effect reaches. This electrical double layer is called Debye length and is why a particle can generate different hydrodynamic diameters in different solvents. The solvent used in this project was a phosphate buffer containing small amounts of Mg^{2+}, Cl^{2+}, and Fe^{2+} ions to more closely represent a biological environment and a gram-negative bacteria growth medium.[40]

Hydrodynamic diameters given by the software for DLS measurements of these star polymers are rather inaccurate because of aggregation. It would have been ideal to compare the Z-average values obtained from the software. However, the DLS samples were partly aggregated, so the Z-averages are biased towards the aggregates and are therefore quite useless for comparison of the actual sizes of the star polymers. As an example, Z-averages obtained were as big as 700 nanometres in some cases. With some of the polymers, aggregation also affected volume and number-weighed hydrodynamic diameters, which makes those volume and number-weighed diameters provided by the software useless as well. All the samples were filtered with a 0.2 μm syringe filter, yet aggregates bigger than this were observed. This leads to thinking that aggregation must happen after filtration.

As the star polymer sizes can not really be compared using Z-averages or intensity, volume, or number-weighed hydrodynamic diameters provided by the software, another method has to be used for the comparison. Intensity, volume, and number-based harmonic means were calculated using equation **3** (Table **2**). In these calculations, only the data of the first peak was taken into account to minimise the effect of aggregates. Having to use own calculations is not as optimal as the Z-averages would have been, but nevertheless allows an indicative comparison between the star polymers. Polymer **8f** is probably the only one of which Z-average is not biased as no aggregation can be seen from the measurement graphs (Figure **14**). Comparing this Z-average value (58.06 nm ± 0.24 nm) to the calculated intensity-based harmonic mean (57.99 nm ± 0.63 nm) shows a good correlation, so the results from these calculations should be reliable enough to use.

$$D = \frac{\sum S_i}{\sum \frac{S_i}{D_i}}$$ **(3)**

S_i = the intensity of scattered light from particle i
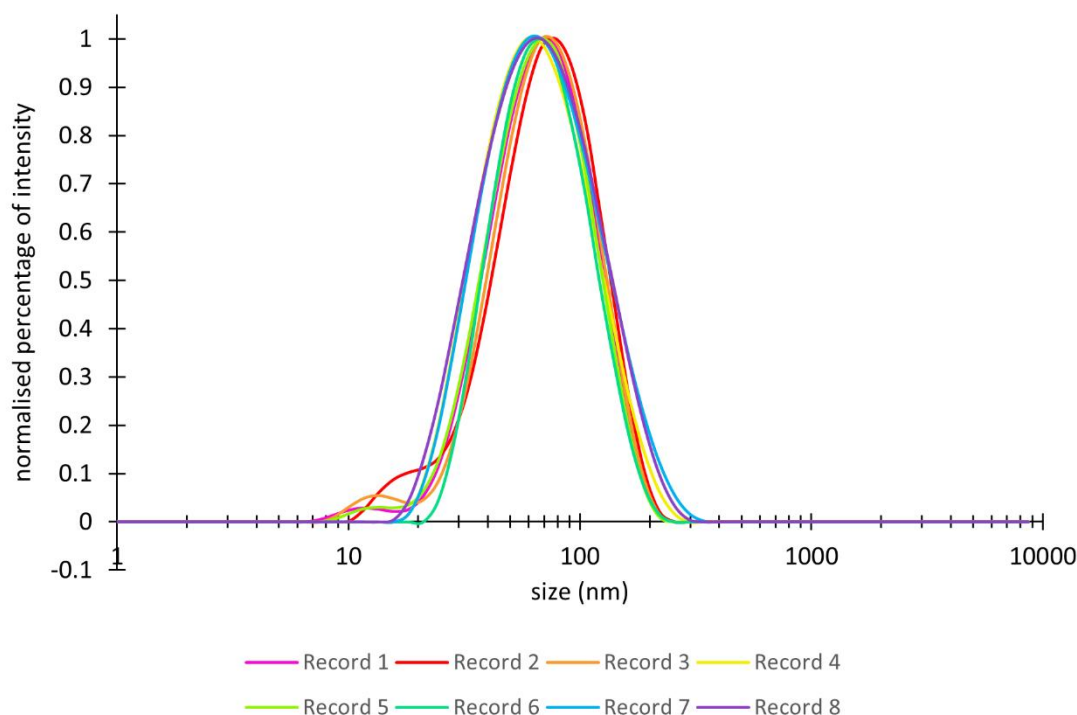
D_i = the diameter of particle i

Figure 11: Size distribution by intensity of product **8f**.

Table 2: Intensity, volume, and number-based diameters of star polymers **8a**–**8g** obtained from equation **3**, and their Z-averages from Zetasizer.

polymer	Z-average from Zetasizer (nm)	intensity-based diameter (nm)	volume-based diameter (nm)	number-based diameter (nm)
8a	63.85 ± 2.81	50.83 ± 0.70	33.68 ± 0.50	27.91 ± 0.59
8b	66.21 ± 2.31	57.63 ± 0.68	30.08 ± 0.97	23.24 ± 0.90
8c	577.6 ± 45.69	57.79 ± 10.65	52.17 ± 11.81	42.36 ± 8.40
8d	79.48 ± 3.93	61.60 ± 0.86	34.71 ± 1.85	16.45 ± 0.65
8e	734.9 ± 40.09	51.98 ± 7.81	49.53 ± 6.56	45.82 ± 6.23
8f	58.06 ± 0.24	57.99 ± 0.63	30.14 ± 0.75	23.21 ± 0.67
8g	67.30 ± 0.27	60.90 ± 0.81	16.78 ± 2.17	12.49 ± 1.83

The number and volume-based results are not as biased towards aggregates. The intensity distribution is 10^6-fold highlighted for bigger particles, whereas the volume distribution is only 10^3-fold highlighted, and the number distribution describes the relative amounts of each species in the solution. When comparing the number distributions to the intensity distributions, it is clear that only a very small part of the polymers is actually aggregated (Figure **15**), but unfortunately, that is enough to corrupt the Z-averages. There are two exceptions, however. Polymers **8c** and **8e** seem to be aggregated more than the others (Figure **16**). This is also obvious in the standard errors of the calculations. These two samples were measured again but with lower concentrations. Aggregation was still prominent, but measurement quality worsened, so lowering concentration did not really reduce aggregation.
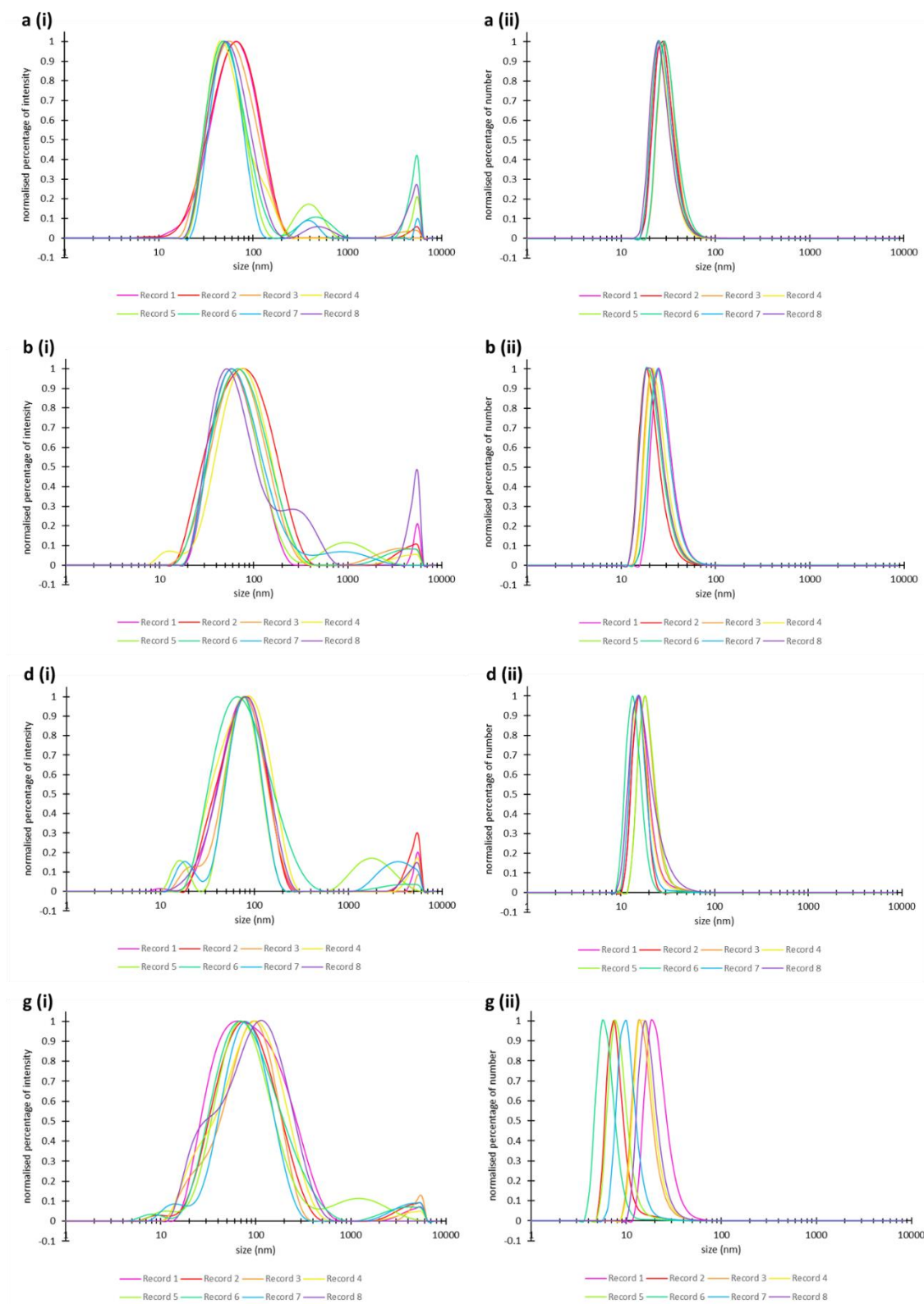
Figure 12: Size distributions by intensity **(i)** and number **(ii)** of star polymers **8a**, **8b**, **8d**, and **8g**.
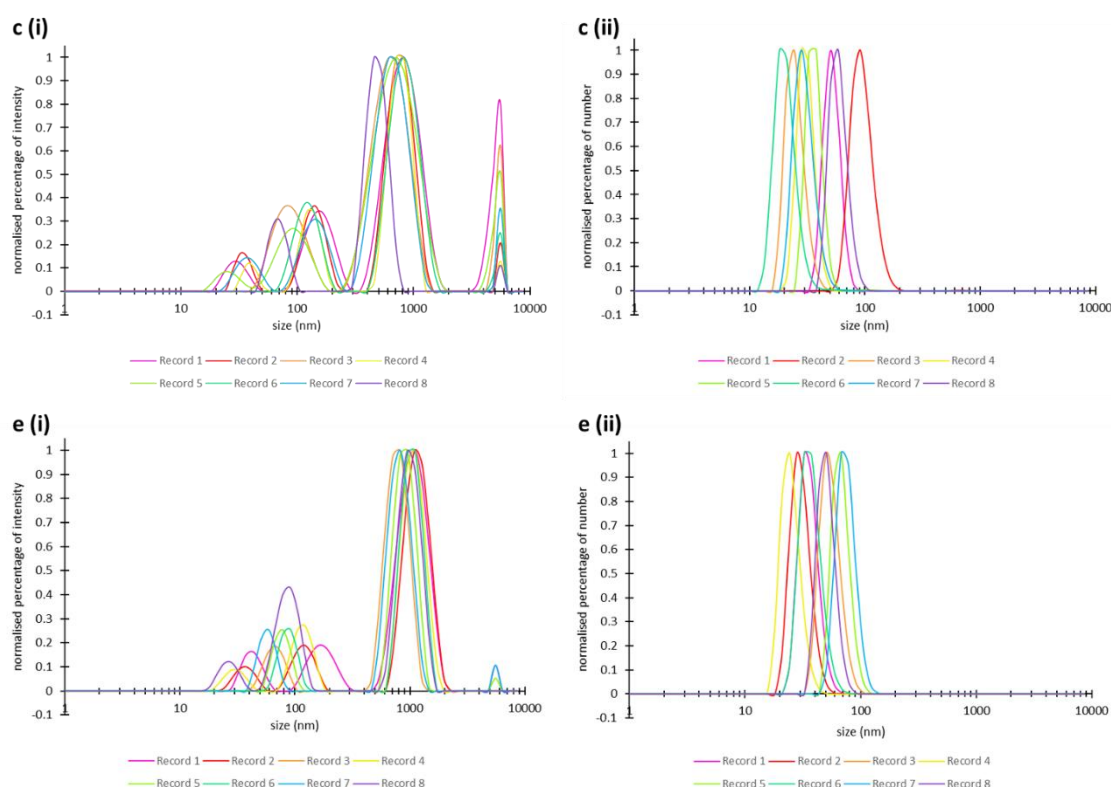
Figure 13: Size distributions by intensity **(i)** and number **(ii)** of star polymers **8c** and **8e**.

Another thing that can be noticed when comparing the intensity, volume, and number distributions is that the volume and number-based diameters are smaller than the intensity-based diameters. This tells that the star polymers are quite polydisperse since in the optimal case where the sample is perfectly monodisperse, all the diameters would be the same. As mentioned before, this heterogeneity is probably due to the viscous reaction mixtures. It is notable, though, that the intensity distribution is converted to volume and number distributions by the software using the refractive index. The value used in these measurements was found in the literature.[72] However, it was for a comb-like POEGMA polymer and not for star polymers, so it is unsure if this has affected the two latter distributions.

In retrospect, it could have been helpful to perform measurements with lower concentrations of all the polymers and not just of the two most aggregated ones. Perhaps less aggregation would have occurred in this case. Alternatively, it would have been interesting to see the results obtained with unfiltered samples, as filtering seems to be the main reason for aggregation. The problem with this is that any specks of dust would make the results even worse. Now, unfortunately, no exact Z-average

hydrodynamic diameters were obtained. However, these results do provide somewhat approximate vicinities on which future decisions regarding a suitable degree of polymerisation can be based. Additionally, the eventual goal is to conjugate star polymers to colicin proteins, so the sizes of these conjugates are ultimately more important than the sizes of bare star polymers. However, it is safe to say as the degree of polymerisation increases, the rate of increase in diameter decreases. This is expected since, with longer polymer chains, there is more space between the arms for the chains to coil. It might be interesting to try one polymerisation reaction with significantly larger monomer amounts and see if the bare star polymers can actually get much bigger.

2.4.2 End group conversions
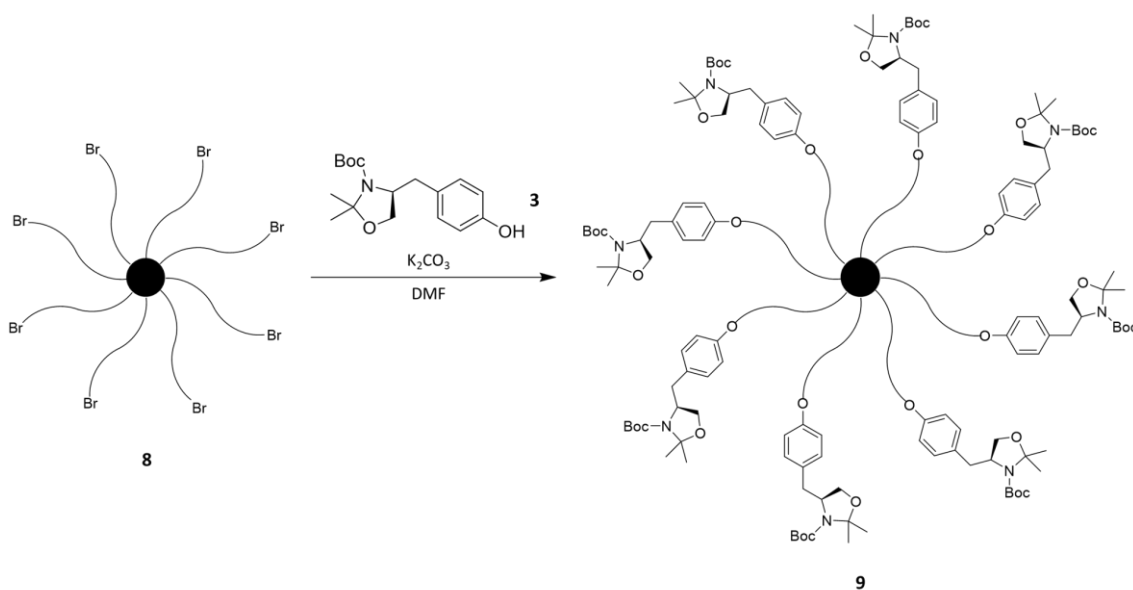
Scheme 10: End group linker attachment to star polymers.

The end group linker was attached to three of the star polymers using the same method as with the linear polymer. Unfortunately, the molecules are so large and contain so many protons that the characteristic aromatic protons are not visible even in the NMR spectrum of the smallest star polymer. There is, however, some increase in the peaks at around 1 ppm, which could correspond to the methyl groups of the protecting groups. Regardless, definite characterisations were not achieved to confirm the success of the reaction. As the same reaction had worked for the linear polymer, it was hoped that the

reaction had occurred with star polymers as well, and for this reason, the following end group modifications were attempted.
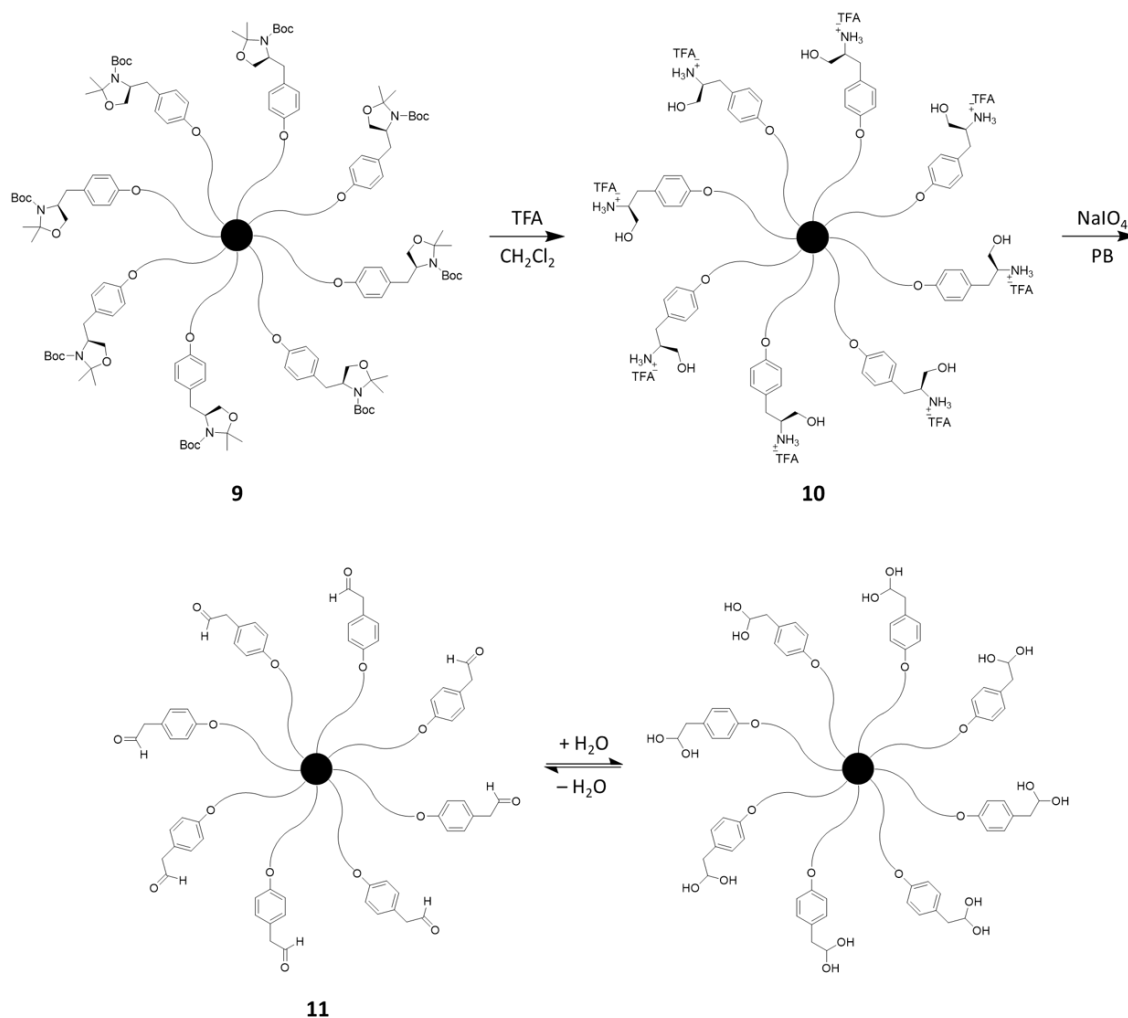

Scheme 11: End group modifications of products **9**.

End group modifications of products **9** were performed using the same method as with the linear polymer. Again, the characteristic protons are not visible in the NMR spectra, although after the first step, there is some decrease in the number of peaks around 1 ppm, which could result from the removal of the protecting groups. The aldehyde proton peaks of the final products are not visible. It is hoped that the reactions have worked since they worked for the linear polymer. Even though no final characterisations were achieved, OPAL reactions were tried on these polymers in hopes that if the occurrence of OPAL reactions could be confirmed, that would also confirm the success of the end group attachment and conversions.

2.5 Myoglobin oxidation

Myoglobin was used as a model protein in this project. It was oxidised to introduce an α-oxo-aldehyde functionality into the protein. This is needed for OPAL reactions, as the reaction intermediate formed by organocatalyst and aldehyde donor will react with the protein aldehyde.[68] Aldehyde introduction is easily achieved with myoglobin because it naturally has a glycine as *N*-terminal amino acid, which can be turned into an aldehyde by successive transamination and oxidative deamination reactions.
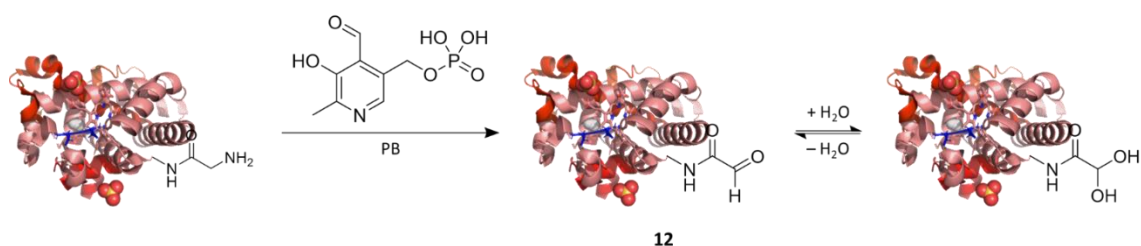
Scheme 12: Synthesis of glyoxyl-myoglobin (**12**).

Myoglobin was oxidised to glyoxyl-myoglobin using a method from the literature.[73] The product was synthesised successfully, although the yield remained relatively low because some of the product precipitated during dialysis. This resulted in a relatively low-concentrated product solution. Product **12** was characterised by UV-Vis spectroscopy and mass spectrometry. Mass spectrometry confirmed the success of the reaction as molecular weights for both aldehyde (M = 16 950 g mol^{-1}) and hydrate (M = 16 968 g mol^{-1}) forms are visible in the mass spectrum (Figure **17**). The peak corresponding to the aldehyde form is expectedly smaller as the hydrate is anticipated to be the dominant form. UV-Vis spectrum was recorded to see if the characteristic peak at approximately 410 nm would remain after the reaction (Figure **18**). This peak corresponds to the heme group of myoglobin, and the disappearance of this peak would mean that the heme group had been detached. This, in turn, would have resulted from myoglobin denaturation, because of which weak interactions binding heme would have been broken. It is crucial to know that the protein retains its tertiary structure throughout the reaction as otherwise it would not be functional anymore. The aromatic residues of myoglobin are also visible in the UV-Vis spectrum at around 280 nm. UV-Vis was also used to determine the concentration of the product solution using the Beer-

Lambert Law (equation **4**).

$$A = \varepsilon cl \tag{4}$$

A = absorbance (obtained from the UV-Vis measurement

ε = the molar attenuation coefficient of the attenuating species (188 mM^{-1} cm^{-1} for myoglobin[74])

c = the concentration of the attenuating species
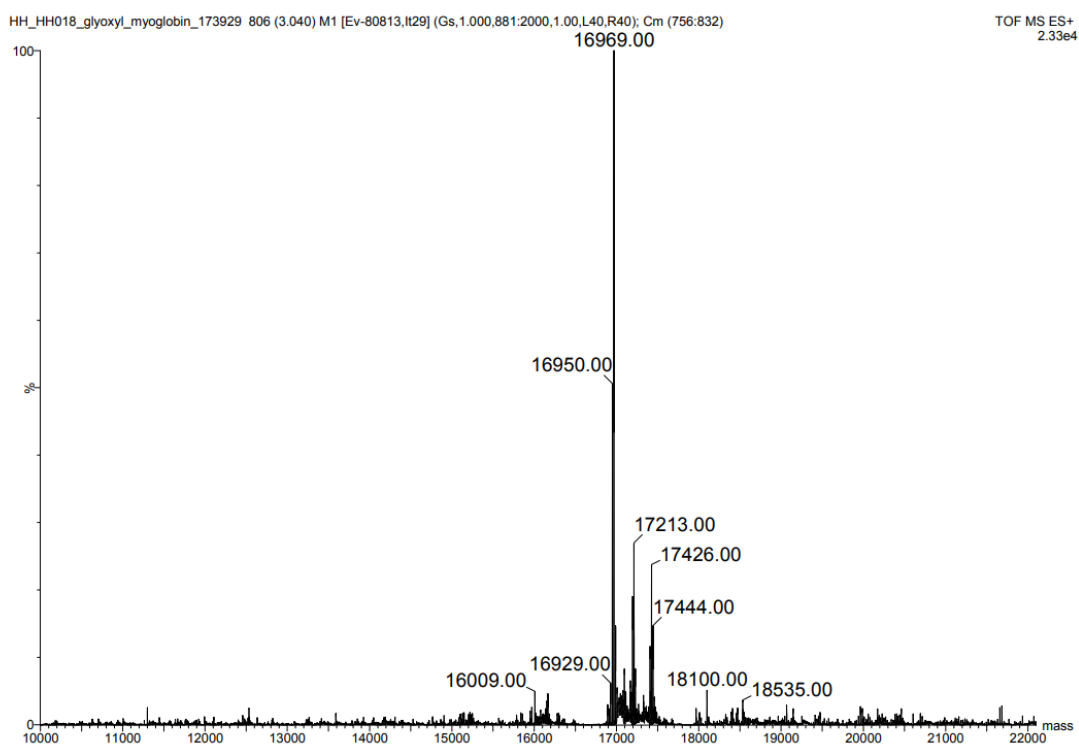
l = the length of the optical path

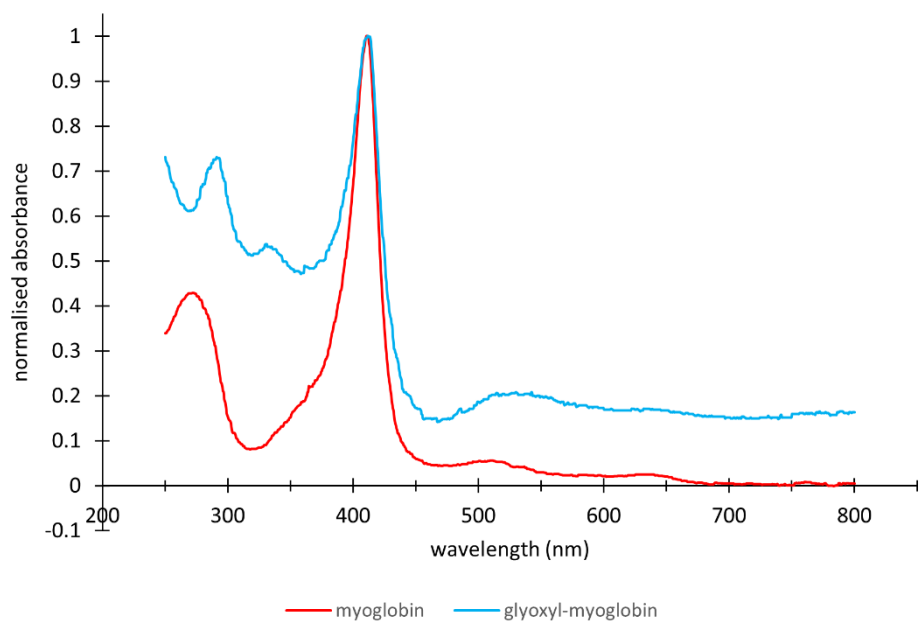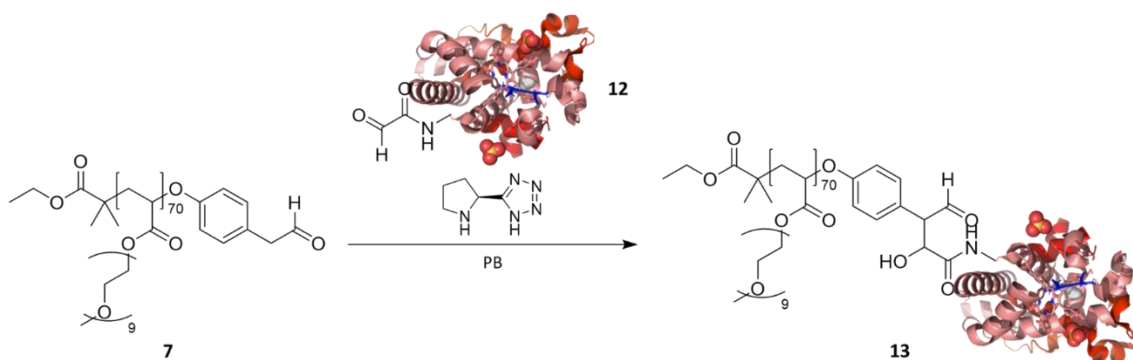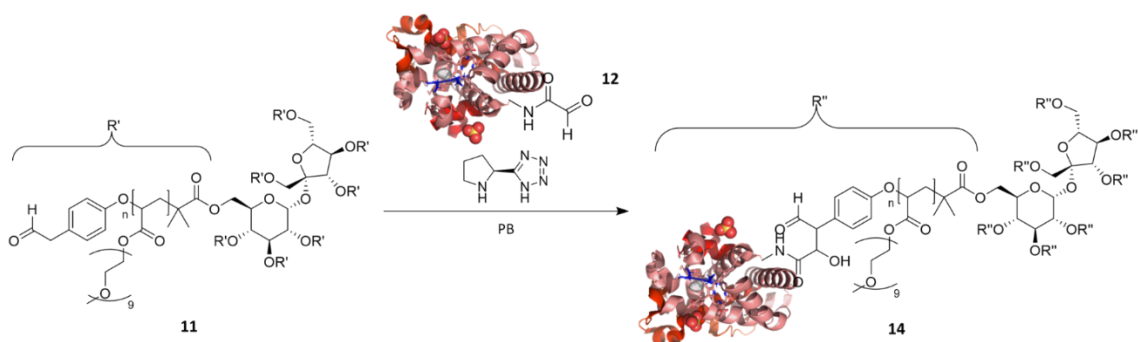**Figure 14:** Mass spectrum of glyoxyl-myoglobin (**12**).

Figure 15: UV-Vis spectra of myoglobin and glyoxyl-myoglobin (**12**).

2.6 OPAL reactions

OPAL reactions were performed according to a method from the literature.[68] They were tested on the linear polymer and three of the star polymers (Table **3**).

Scheme 13: OPAL reaction between the linear polymer **7** and glyoxyl-myolobin (**12**).

Scheme 14: OPAL reaction between a star polymer and glyoxyl-myoglobin (**12**).

In the literature method, 250 equivalents of aldehyde donor are used compared to the amount of glyoxyl-myoglobin. However, in this project, the aldehyde donor is the polymer, so such excess could not be used as there was not enough polymer. Even if there was, characterisations would be nearly impossible as such big polymers would dominate all the measurements. Instead, different equivalent combinations were tested on linear polymers. Because of the reference method, bigger equivalents of the linear polymer ended up being used in two of the reactions, but in the future, it would also be interesting to try the reactions with bigger equivalents of glyoxyl-myoglobin. In this reaction, not enough product was obtained to be used in large excesses, and the concentration of the glyoxyl-myoglobin solution remained low, so excessive use would have resulted in big reaction mixture volumes. With star polymers, the amount of glyoxyl-myoglobin and, therefore, the volume of the reaction mixture was dictated by how much solvent was required to get the polymers to dissolve. The products were characterised by DLS, GPC, and SDS-PAGE.

Table 3: OPAL reactions tried in this project.

OPAL reaction	OPAL product	polymer used	amount of glyoxyl-myoglobin used	amount of polymer used
1	**13**	**7**	1 eq	2 eq
2	**13**	**7**	2 eq	1 eq
3	**13**	**7**	1 eq	1 eq
4	**13**	**7**	1 eq	10 eq
5	**13**	**7**	1 eq	35 eq
6	**14a**	**11a**	2 eq per arm	1 eq
7	**14f**	**11f**	8 eq per arm	1 eq
8	**14g**	**11g**	8 eq per arm	1 eq

Gel Permeation Chromatography (GPC)

Provided the reaction has worked, the size of the product should be bigger than the sizes of the starting materials. GPC measurements of reactions 1, 2, and 6 were performed to investigate this (Figure **19**). The results do not show any apparent differences in retention times between the starting materials and the product. However, it is expected that the reaction would not have occurred quantitatively, in which case the sample would contain three different-sized molecules. For reactions 1 and 2, all three molecules would have sizes and, therefore, retention times very close to each other. So it is possible that instead of three peaks, we would see them all as one fused peak, and all three particles would have contributed to its retention time. Accordingly, based on these results, nothing really can be said about the OPAL reactions.
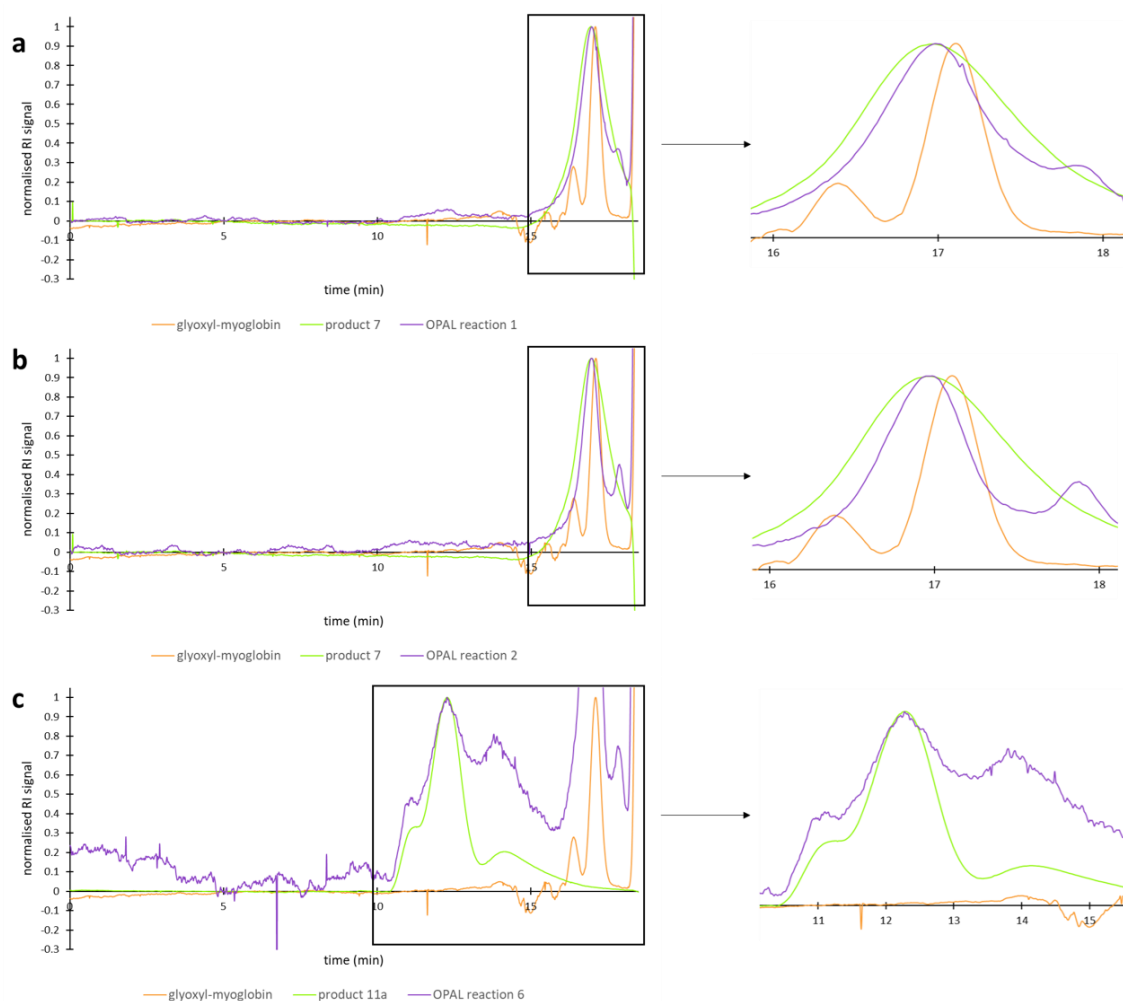
Figure 16: GPC spectra of **(a)** OPAL reaction 1, **(b)** OPAL reaction 2, and **(c)** OPAL reaction 6.

Dynamic Light Scattering (DLS)

DLS measurements were performed for the same reason as GPC measurements: to find out if particle size has increased, which should have happened if the reactions have worked. Intensity, volume, and number-based harmonic means were again calculated using equation **3** (Table **4**). First of all, the sizes of the myoglobin and the linear polymer are approximately 4 nm and 7 nm, respectively, so it is not expected that the size of the conjugate formed by them would be hundreds of nanometres. Therefore, it can be concluded that the samples have aggregated again, and the volume and number distributions are most likely closer to the actual sizes of the conjugates if they have been formed.

43

Table 4: Intensity, volume, and number-based diameters of OPAL reactions 1–8 obtained from equation **3**.

DLS sample	intensity-based diameter (nm)	volume-based diameter (nm)	number-based diameter (nm)
myoglobin	4.15 ± 0.13	3.80 ± 0.10	3.63 ± 0.11
product **7**	7.32 ± 0.11	6.21 ± 0.07	5.55 ± 0.12
OPAL reaction **1**	37.93 ± 7.04 497.1 ± 62.4	45.07 ± 6.32 503.5 ± 61.0	42.66 ± 5.83 437.2 ± 58.3
OPAL reaction **2**	252.2 ± 5.8	245.6 ± 6.2	234.4 ± 5.4
OPAL reaction **3**	45.94 ± 3.94 505.5 ± 35.6	41.88 ± 3.02 513.6 ± 34.7	38.95 ± 2.47 456.2 ± 23.9
OPAL reaction **4**	7.22 ± 0.15	5.96 ± 0.05	5.31 ± 0.09
OPAL reaction **5**	7.06 ± 0.09	6.04 ± 0.16	5.56 ± 0.15
product **11a**	50.83 ± 0.70	33.68 ± 0.50	27.91 ± 0.59
OPAL reaction **6**	86.88 ± 2.08	26.77 ± 0.59	20.53 ± 0.31
product **11f**	58.06 ± 0.24	57.99 ± 0.63	30.14 ± 0.75
OPAL reaction **7**	76.03 ± 5.33 498.9 ± 19.5	67.81 ± 4.47 517.2 ± 21.2	61.88 ± 4.03 415.9 ± 6.4
product **11g**	60.90 ± 0.81	16.78 ± 2.17	12.49 ± 1.83
OPAL reaction **8**	658.3 ± 25.3	660.0 ± 21.3	512.9 ± 22.9

What can be noticed from reactions 1–3 is that the products are bigger than either of the starting materials and even bigger than the starting material polymer aggregates (Figure **20**). This leads to thinking that at least something has occurred during the reaction. The volume and number distributions also show quite big sizes, so the possibility for them to be aggregates as well can not be ruled out. However, with reactions 4 and 5, no bigger-sized particles than starting materials can be observed. This is partly expected since polymer was used in large excesses in both cases, so it would produce the most prominent peak. In reaction 4, the excess is only 10-fold, yet even the number distribution does not show any bigger sizes. Therefore, it can probably be concluded that reactions 4 and 5 have not worked. This is interesting because, in the reference publication, aldehydes were used in excess amounts. Perhaps the polymers benefit more from an excess of glyoxyl-myoglobin, than glyoxyl-myoglobin benefits from an excess of polymers.
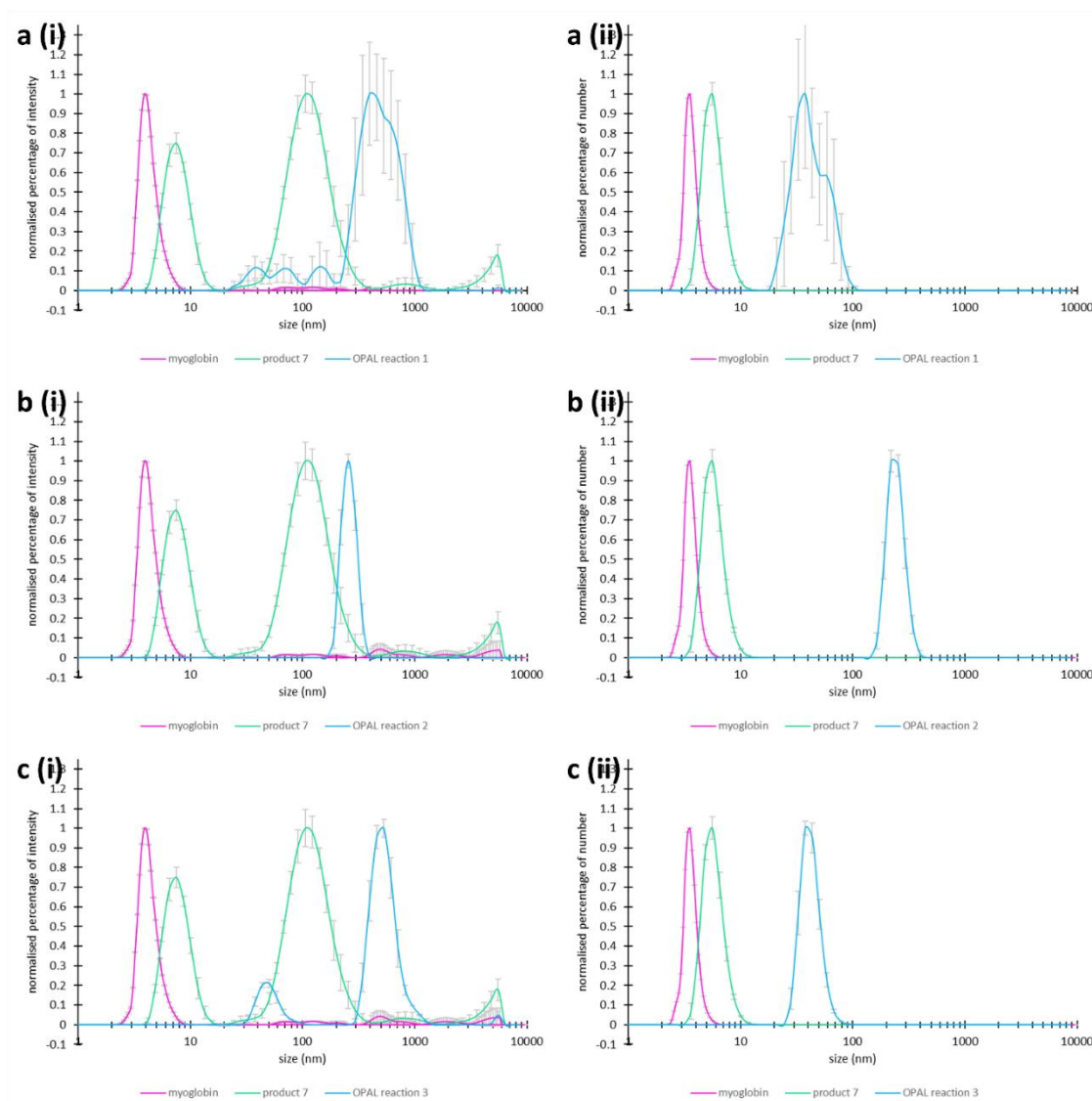
Figure 17: Arithmetic means of size distributions by intensity **(i)** and number **(ii)** of OPAL reactions. **(a)** OPAL reaction 1. **(b)** OPAL reaction 2. **(c)** OPAL reaction 3.

The volume and number distribution of reaction 6 do not demonstrate any peaks corresponding to bigger sizes. In fact, the peaks from the reaction correspond to smaller sizes than the starting material polymer, so it is relatively safe to say that the reaction has not worked. Although it should be remembered that no definite characterisations were obtained for the end group reactions of star polymers, so it is unsure whether the polymer even contains the end group linker or if it has the required aldehyde functionality. What can be said about reactions 7 and 8 is that all the starting materials were completely dissolved at the beginning of the reaction, but after 24 hours, the reaction mixtures contained particles visible to the naked eye. Although nothing reliable can be said with visual analysis, it is clear that something has occurred. They also did not

go through a filter, so DLS measurements were performed on unfiltered samples. The results demonstrate big hydrodynamic diameters again (Figure **21**), although since the samples were unfiltered, it cannot be said for sure if they are aggregates or just dust.
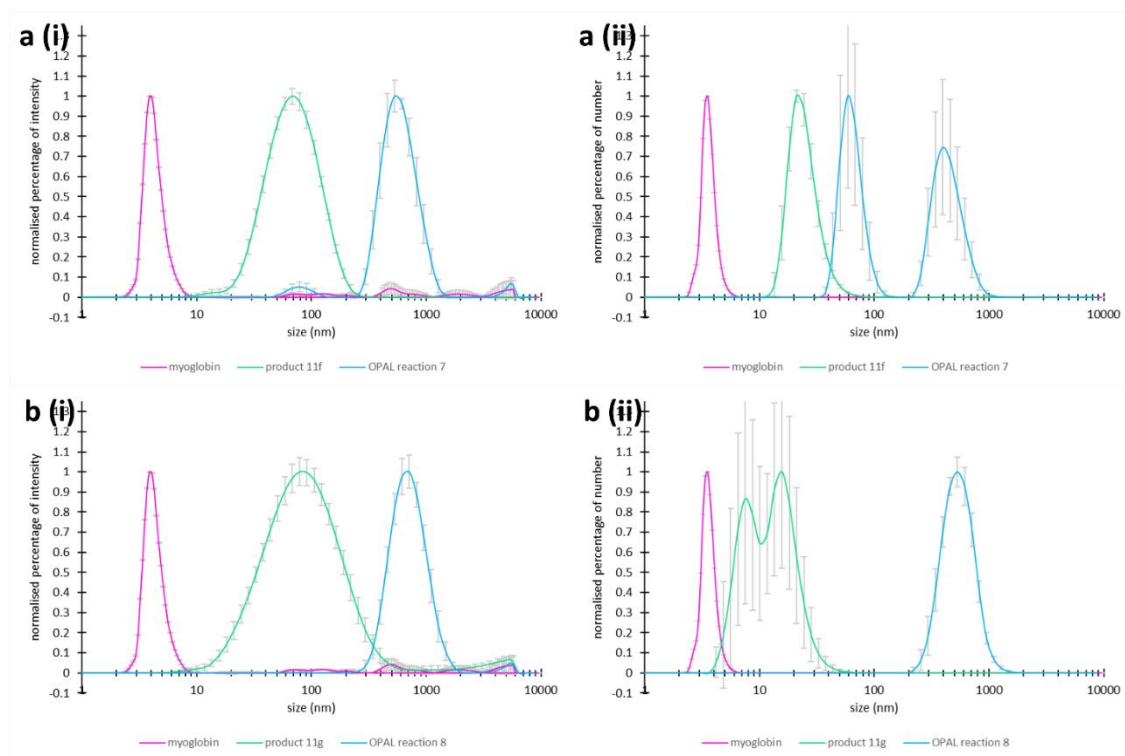

Figure 18: Arithmetic means of size distributions by intensity **(i)** and number **(ii)** of OPAL reactions. **(a)** OPAL reaction 7. **(b)** OPAL reaction 8.

What is surprising is the observation that, especially with reactions 2 (Figure **20b**), 7 (Figure **21a**), and 8 (Figure **21b**), the volume and number distributions demonstrate peaks at the same D_h as the intensity distribution. This means that most of the particles have aggregated, and the aggregates are quite uniform in size. Even though these DLS measurements do not confirm OPAL reactions, they do demonstrate that something has definitely happened, whether it is only extensive polymer aggregation or even micellisation of polymer–protein conjugates.

Sodium Dodecyl Sulphate Polyacrylamide Gel Electrophoresis (SDS-PAGE)

SDS-PAGE is a technique that separates proteins based on their different migration rates in a polyacrylamide gel. Migration is induced by an electrical current which makes the

negatively charged proteins move towards a positively charged anode. In general gel electrophoresis, factors affecting the rate of movement include, for example, the length, molecular weight, and electric charge of the proteins. In SDS-PAGE, however, proteins are denatured with SDS, making their migration only based on their molecular weight. Small proteins fit through the pores of the gel more easily, whereas larger proteins face resistance and move more slowly in the gel. Using references, the size of the samples can be estimated.

SDS-PAGE was hoped to confirm whether OPAL reactions had or had not worked. It is suitable for molecules with molecular weight between 5 and 250 kDa, so it was used for reactions 1–5. The gel was successfully run, but unfortunately, Coomassie staining was not sensitive enough to stain the samples, so more sensitive silver staining could be used in the future. In conclusion, it is unfortunately impossible to say for sure if OPAL reactions have worked even though DLS results show that something has happened.
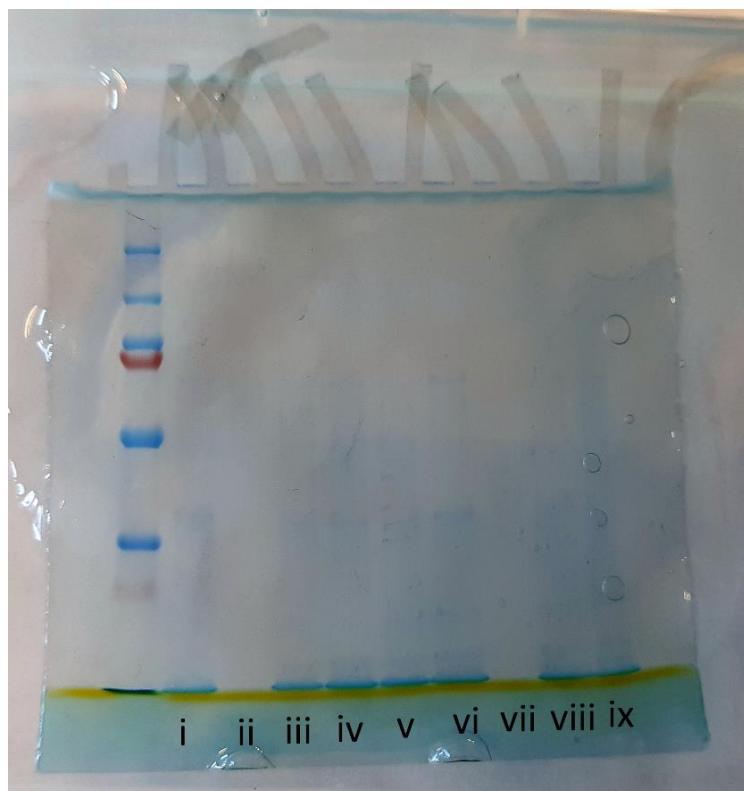
i) myoglobin
ii) product **7**
iii) OPAL reaction 1
iv) OPAL reaction 2
v) OPAL reaction 3
vi) myoglobin
vii) product **7**
viii) OPAL reaction 4
ix) OPAL reaction 5

Figure 19: SDS-PAGE gel of myoglobin, product **7**, and OPAL reactions 1–5 stained with Brilliant Blue G solution.

2.7 Conclusions and future directions

A sucrose-based initiator and an end group linker were synthesised successfully and characterised by ^{1}H NMR and ^{13}C NMR spectroscopy, and mass spectrometry. One linear polymer and eight star polymers of various sizes were successfully synthesised by single-electron transfer living radical polymerisation (SET-LRP). Viscous reaction mixtures made the optimisation of reaction conditions difficult and have most likely resulted in ununiform products. Degrees of polymerisation were determined by ^{1}H NMR conversion analysis and sizes by dynamic light scattering (DLS). Aggregation of star polymers significantly complicated the DLS studies, and the sizes obtained are more indicative than exact hydrodynamic diameters. Gel permeation chromatography (GPC) measurements were performed to indicate the dispersities of synthesised polymers, but unfortunately, all the star polymers exceeded the column calibration limits and therefore did not provide very useful information. End-group attachment and conversions were performed on both the linear polymer and three star polymers. With the linear polymer, these reactions were confirmed by ^{1}H NMR, as aromatic peaks demonstrate the presence of the linker, and an aldehyde peak confirms the conversions into the final product. However, star polymers produce such dominant polymer peaks that a definite confirmation of the success of the reactions was not achieved. Nevertheless, there are minor changes that might correspond to the end-group linker's methyl groups and then the disappearance of these methyl groups. The project was carried on with these products because it was hoped that the reactions had worked as they had worked for identically synthesised linear polymer. Next, myoglobin was oxidised to glyoxyl-myoglobin. Mass spectrometry confirmed the reaction, and UV-Vis spectrometry confirmed that the protein had not denatured. Finally, OPAL reactions between polymers and glyoxyl-myoglobin were tried with various equivalents of starting materials. Gel electrophoresis was hoped to confirm of the success of these reactions. Unfortunately, Coomassie staining was not sensitive enough to stain the samples. However, DLS studies indicate bigger particles than either of the starting materials, which is promising. Again, aggregation is observable, and the percentage of that is much greater than with bare star polymers, which might possibly be due to micellisation.

In the future, a more sensitive silver staining method could be used for electrophoresis first to confirm the success of OPAL reactions. Then the reaction conditions should be optimised for these conjugation reactions. After this, star polymers could be conjugated to functionalised colicin proteins. Attaching a fluorophore to these conjugates would allow studying their binding and effect on *E. coli* outer membrane protein movement in the outer membrane. This would finally demonstrate whether star polymer–protein conjugates could potentially act as antibiotic agents in the future.

3 Experimental

3.1 General procedures

Mass Spectrometry (MS)

Measurements were performed by either Dr. David Parker or Mr. Peter Stokes of the Durham University Mass Spectrometry Service using Waters Ltd QToF Premier mass spectrometer and an Acquity UPLC for small molecules, and Waters Ltd Xevo QToF mass spectrometer for proteins.

Nuclear Magnetic Resonance (NMR) spectroscopy

^{1}H NMR and ^{13}C NMR spectra were recorded either on Bruker Neo-400 spectrometer with operating frequencies of 400.20 MHz for ^{1}H and 100.63 MHz for ^{13}C, or on Bruker Avance III-HD-400 spectrometer with operating frequencies of 400.07 MHz for ^{1}H and 100.60 MHz for ^{13}C. Chemical shifts are reported in ppm.

Gel Permeation Chromatography (GPC)

Measurements were performed by Mr. James Cresswell using an Agilent 1260 instrument equipped with a differential refractive index detector and a pair of PL aquagel-OH 8μm Mixed-M columns (300 x 7.5 mm) with a guard column (Polymer Laboratories Inc.) in series. GPC was conducted with PBS (Phosphate Buffered Saline) eluent at 35 °C with a flow rate of 1 mL min^{-1}. Molecular weights were determined through narrow standard calibration (PEG/PEO standards) using the Agilent Infinity software. Samples were made up at 5 mg mL^{-1} in PBS and passed through a 0.2 μm nylon syringe filter prior to analysis.

Dynamic Light Scattering (DLS)

Measurements were performed at 37 °C using a Malvern Zetasizer µV instrument. Samples were made up at 5 mg mL^{-1} in a phosphate buffer and passed through a 0.2 µm syringe filter prior to measurements. Refractive indices of 1.52[72] and 1.33[75] for polymers and myoglobin, respectively, were used to transform intensity distributions to volume and number distributions.

buffer pH	buffer concentration	[Na$_2$HPO$_4$]	[KH$_2$PO$_4$]	[NaCl]	[MgSO$_4$]	[CaCl$_2$]	[FeSO$_4$]
7.2	70 mM	48 mM	22 mM	8.6 mM	2 mM	0.1 mM	0.1 mM

Ultraviolet-visible light (UV-Vis) spectroscopy

UV-Vis spectra were recorded on a Jenway 67 UV/Visible Scanning Spectrophotometer scanning between 250 and 800 nm. Samples were dissolved in a phosphate buffer and the spectra were measured against a reference sample of this phosphate buffer.

| buffer pH	buffer concentration	[Na$_2$HPO$_4$]	[KH$_2$PO$_4$]
7.5	25 mM	17 mM	8 mM

Centrifugation

Centrifugation was performed using a Sigma 2-5 centrifuge at 2000 rpm.

**Sodium dodecyl sulphate polyacrylamide gel electrophoresis (SDS-PAGE)**

Cleaver Scientific omniPAGE Mini package was used for gel electrophoresis. The resolving gel was a 12% acrylamide gel ran at 150V voltage.

3.2 Synthesis of sucrose-based intiator octakis-*O*-(2-bromoisobutyryl)-sucrose
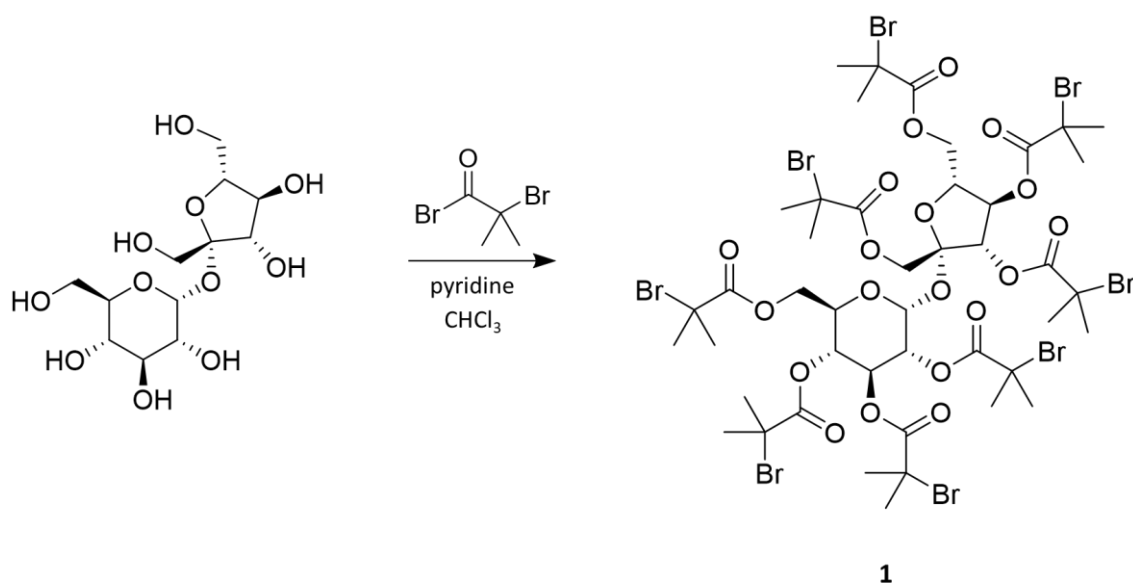
A sucrose-based initiator **1** was synthesised using a method from the literature.[70] Sucrose (1.00 g, 2.92 mmol, 1 eq) was dissolved in anhydrous pyridine (30 mL). 2-bromoisobutyryl bromide (5.42 mL, 43.8 mmol, 15 eq) was dissolved in anhydrous chloroform (30 mL). The 2-bromoisobutyryl bromide solution was added dropwise to the sucrose solution, resulting in an instantaneous formation of a yellow solid. The reaction mixture was heated at reflux under an argon atmosphere for 3 hours, resulting in a dissolution of the yellow solid. The reaction mixture was the stirred overnight at room temperature. The solution was washed with ice cold deionised water (150 mL), aqueous NaOH solution (0.1 M, 100 mL) and brine (100 mL). The organic phase was collected and dried with anhydrous $MgSO_4$. The solvent was removed *in vacuo* to yield a brown solid. After 6 recrystallisations from methanol, product **1** was afforded as a white solid (1.44 g, 32 %).

¹H NMR δ$_H$ (400 MHz, CDCl$_3$): 5.80 (1H, d, *J*=3.8 Hz, H6), 5.72 (1H, d, *J*=8.4 Hz, H9), 5.65 (1H, dd, *J*=9.8 Hz, *J*=10.1 Hz, H4), 5.60 (1H, dd, *J*=8.3 Hz, *J*=8.9 Hz, H10), 5.32 (1H, dd, *J*=9.8 Hz, *J*=10.1 Hz, H3), 5.08 (1H, dd, *J*=3.8 Hz, *J*=10.2 Hz, H5), 4.77 (1H, dt, *J*=1.8 Hz, *J*=10.3 Hz, H2), 4.63 (1H, dd, *J*=1.6 Hz, *J*=12.9 Hz, H7'), 4.31–4.46 (5H, m, H1, H7'', H11, H12'), 4.09 (1H, d, *J*=11.8 Hz, H12''), 1.76–1.98 (48H, m, H15); **¹³C NMR** δ$_c$ (400 MHz, CDCl$_3$): 169.6–171.3 (C13), 102.6 (C8), 88.7 (C6), 77.2 (C11), 75.8 (C2), 73.6 (C3), 70.9 (C10), 70.7 (C9), 68.5 (C4), 68.2 (C5), 64.7 (C1, C7, C12), 54.1–55.7 (C14), 30.2–30.9 (C15); **ESI-MS** most abundant mass: found 1531.814, calculated 1531.73; **m.p.**: 130–132 °C (literature value 131–133 °C[69]).
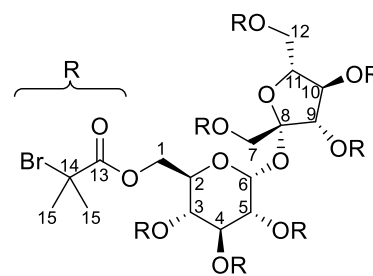
3.3 Synthesis of end group linker

The end group linker **3** was synthesised using a two-step method from the literature.[68]
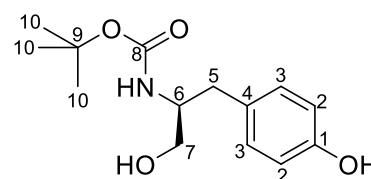
3.3.1 Synthesis of (*S*)-*tert*-butyl-(1-hydroxy-3-(4-hydroxyphenyl)-propan-2-yl)carbamate


2
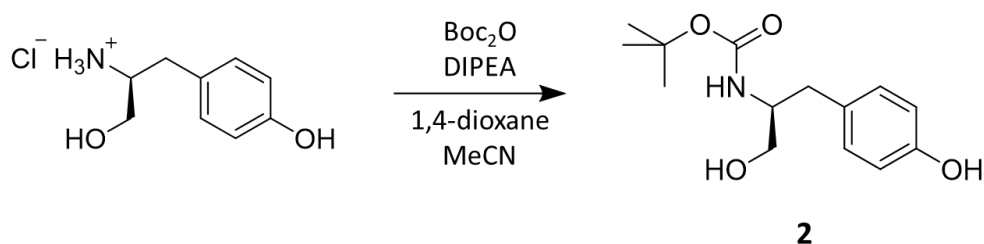
L-tyrosinol hydrochloride (1.10 g, 5.40 mmol, 1 eq) and di-*tert*-butyl dicarbonate (1.17 g, 5.4 mmol, 1 eq) were added to a Schlenk tube. Reagents were dried *in vacuo* and the tube was filled with argon. 1,4-dioxane (10 mL) and di-isopropyl ethyl amine (1.88 mL, 2 eq) were added to the tube. The starting material did not dissolve so acetonitrile (2 mL) was added. The reaction mixture was stirred for 45 minutes but some of the starting material still remained undissolved. More acetonitrile was added (2 mL) and the reaction

mixture was stirred for another 45 minutes. All starting material had finally dissolved so the reaction mixture was stirred overnight under an argon atmosphere. TLC analysis (ethyl acetate/*n*-hexane 1:1) showed full conversion of the starting material. The solvent was removed *in vacuo* to yield a colourless oil. The oil was dissolved in ethyl acetate (20 mL) and washed with aqueous citric acid solution (5 % w/v; 50 mL) and deionised water (50 mL). The organic layer was collected and dried over anhydrous MgSO₄ after which the solvent was removed *in vacuo*. The crude product was purified by silica gel column chromatography (ethyl acetate/*n*-hexane 1:1). Solvent removal in vacuo afforded the product **2** as a white solid (0.95 g, 67 %).

¹H NMR δ_H (400 MHz, CD₃OD): 8.92 (s, C1-OH), 6.92 (2H, d, *J*=8.2 Hz, H3), 6.59 (2H, d, *J*=8.2 Hz, H2), 6.20 (d, *J*=8.5 Hz, NH) 5.22 (br, C7-OH), 3.58 (1H, ddt, *J*=5.7 Hz, *J*=6.0 Hz, *J*=7.2 Hz, H6), 3.36 (2H, m, H7), 2.64 (1H, dd, *J*=6.2 Hz, *J*=13.7 Hz, H5'), 2.46 (1H, dd, *J*=7.8 Hz, *J*=13.6 Hz, H5''), 1.26 (9H, s, H10); **¹³C NMR** δ_c (400 MHz, CD₃OD): 156.7 (C1), 155.4 (C8), 129.9 (C3), 129.3 (C4), 114.7 (C2), 78.6 (C9), 63.0 (C7), 54.1 (C6), 36.2 (C5), 27.4 (C10); **ESI-MS** ([M+H]⁺, C₁₄H₂₂NO₄⁺): found 268.1546, calculated 268.1549; **m.p.**: 118–120 °C (literature value 118–119 °C[76]); **R$_f$** (EtOAc/*n*-hexane 1:1): 0.39.

### 3.3.2 Synthesis of (*S*)-*tert*-butyl-4-(4-hydroxybenzyl)-2,2-dimethyl-oxazolidine-3-carboxylate
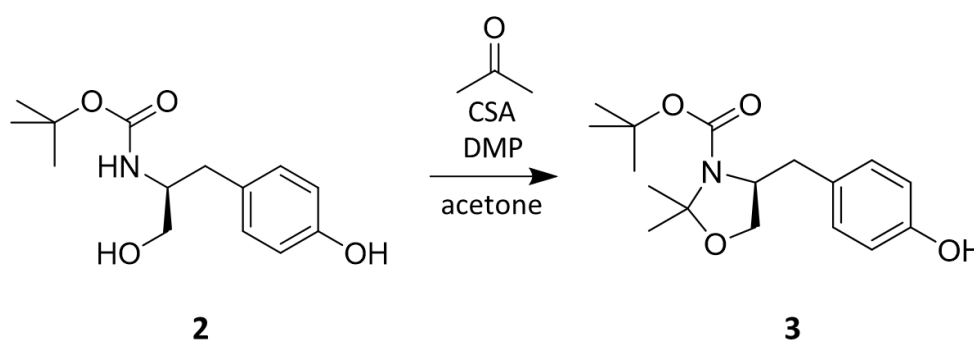
Product **2** (0.50 g, 1.87 mmol, 1 eq) was dissolved in anhydrous acetone (5.45 mL, 74.3 mmol, 40 eq). 10-camphorsulfonic acid (0.0087 g, 0.037 mmol, 0.02 eq) and 2,2-dimethoxypropane (0.70 mL, n = 5.61 mmol, 3 eq) were added. The reaction mixture was stirred at room temperature for 3.5 hours. TLC analysis (ethyl acetate/*n*-hexane 1:3) confirmed complete conversion. The reaction mixture was neutralised with triethylamine and the solvent was removed *in vacuo*, resulting in a colourless oil. The crude product was purified by silica gel column chromatography (ethyl acetate/*n*-hexane 1:3). Solvent removal *in vacuo* afforded the product **3** as a white solid (0.88 g, 81 %).

¹H NMR δ_H (400 MHz, CDCl₃): 7.00 (2H, dd, *J*=8.1 Hz, *J*=15.3 Hz, H3), 6.70 (2H, dd, *J*=8.1 Hz, *J*=13.3 Hz, H2), 5.47 (1H, br d, *J*=17.2 Hz, OH), 3.84–4.01 (1H, m, H6), 3.70 (2H, m, H7), 2.99 (1H, dd, *J*=12.2 Hz, *J*=38.5 Hz, H5'), 2.53 (1H, dd, *J*=10.4 Hz, *J*=13.14 Hz, H5''), 1.45 (9H, s, C12), 1.39–1.64 (6H, m, C9); **¹³C NMR** δ_C (400 MHz, CDCl₃): 154.5 (C1), 152.1 (C10), 130.5 (C3), 130.3 (C4), 115.5 (C2), 93.9 (C8), 80.2 (C11), 66.0 (C7), 59.3 (C6), 38.2 (C5), 28.6 (C12), 23.3–27.6 (C9); **ESI-MS** ([M–H]⁻, C₁₇H₂₄NO₄⁻): found 306.1695, calculated 306.1705; **m.p.**: 112–113 °C (literature value 112.1–113.3 °C[69]); **R$_f$** (EtOAc/*n*-hexane 1:3): 0.50.
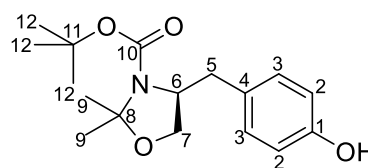
3.4 Synthesis of polymers

Polymers were synthesised using a SET-LRP reaction. Identical reaction methods were used for both the linear polymer and the star polymers.


4
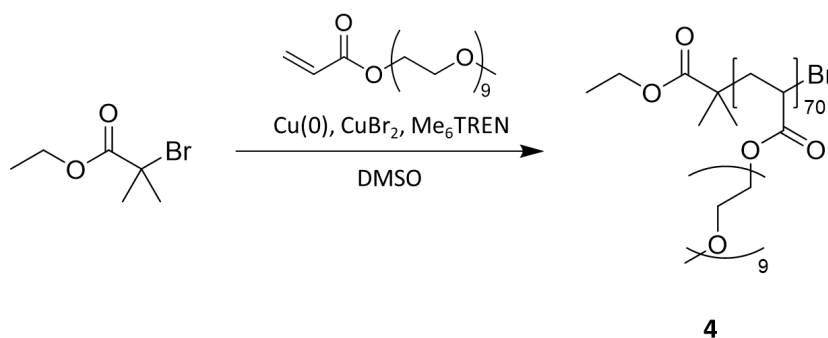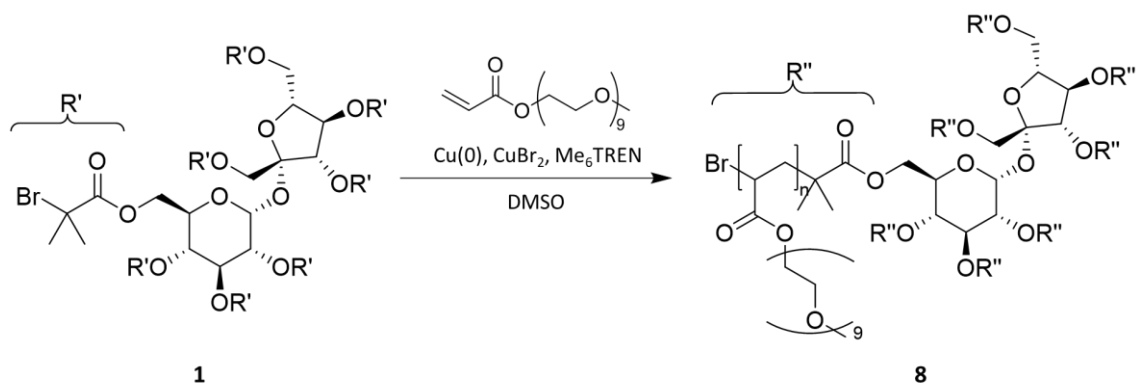
First, poly(ethylene glycol)methyl ether acrylate was passed through a short column of Al_2O_3 to remove radical inhibitors. Ethyl α-bromoisobutyrate/**1**, tris 2-(dimethylamino)ethyl amine, destabilised PEG acrylate, $CuBr_2$, DMSO, and DMF were added to a Schlenk tube. Cu(0) wire wrapped around a stirrer bar was activated by washing with HCl (1 M) and acetone and was dried. This stirrer bar was then held inside the Schlenk tube but above the reaction mixture with a strong external magnet. The tube was sealed and deoxygenated by bubbling argon through the solution for 30 minutes. An NMR reference sample was taken before the reaction was started by dropping the stirrer bar into the solution. The reaction was stirred either overnight (polymers **4** and **8c – 8g**) or until desired conversion percentage was achieved (polymers **8a** and **8b**). NMR samples were taken to indicate conversion percentage. The reaction was quenched by exposing the solution to air and removing Cu(0) wire wrapped around the stirrer bar. The crude polymer was purified by dialysis against high purity water. The polymer was dissolved in a minimum amount of 1,4-dioxane and precipitated by the dropwise addition of this solution to cold hexane (40 mL). Polymer was dissolved in methanol after centrifugation and supernatant decantation. Solvent removal *in vacuo* afforded the products **4** and **8a – 8g** as colourless oils.

| polymer	initiator	monomer	ligand	CuBr$_2$	DMSO	DMF	reacting time	monomer conversion percentage	degree of polymeri-sation per arm (n)	yield
4	V = 7.52 µL	V = 2.26 mL	V = 2.74 µL	m = 2.3 mg	V = 10 mL	V = 100 µL	24 h	70	70	m = 1.23 g
	1 eq	100 eq	0.2 eq	0.2 eq						
8a	m = 1.8 mg	V = 2.87 mL	V = 0.50 µL	m = 0.4 mg	V = 10 mL	V = 100 µL	3 h	62	430	m = 1.99 g
	1 eq	700 eq per arm	0.2 eq per arm	0.2 eq per arm						
8b	m = 1.0 mg	V = 2.87 mL	V = 0.28 µL	m = 0.23 mg	V = 10 mL	V = 100 µL	3.5 h	58	725	m = 0.75 g
	1 eq	1250 eq per arm	0.2 eq per arm	0.2 eq per arm						
8c	m = 1.0 mg	V = 4.59 mL	V = 0.28 µL	m = 0.23 mg	V = 10 mL	V = 100 µL	24 h	54	1090	m = 0.58 g
	1 eq	2000 eq per arm	0.2 eq per arm	0.2 eq per arm						
8d	m = 0.46 mg	V = 2.76 mL	V = 0.11 µL	m = 0.13 mg	V = 10 mL	V = 100 µL	24 h	46	1190	m = 1.61 g
	1 eq	2600 eq per arm	0.2 eq per arm	0.2 eq per arm						
8e	m = 0.6 mg	V = 4.13 mL	V = 0.34 µL	m = 0.7 mg	V = 10 mL	V = 100 µL	24 h	43	1240	m = 0.56 g
	1 eq	3000 eq per arm	0.4 eq per arm	1 eq per arm						
8f	m = 0.3 mg	V = 2.07 mL	V = 0.21 µL	m = 0.35 mg	V = 10 mL	V = 100 µL	24 h	60	1790	m = 1.43 g
	1 eq	3000 eq per arm	0.5 eq per arm	1 eq per arm						
8g	m = 0.2 mg	V = 2.30 mL	V = 0.14 µL	m = 0.34 mg	V = 10 mL	V = 100 µL	24 h	48	2410	m = 0.47 g
	1 eq	5000 eq per arm	0.5 eq per arm	1 eq per arm						

Polymer **4**

¹H NMR δ_H (400 MHz, CD₃OD): 4.16–4.38 (140H, br m, H6), 4.13 (2H, m, H2), 3.71–3.79 (140H, br m, H7), 3.54–3.71 (2240H, br m, H8), 3.37–3.41 (210H, br, H9), 2.19–2.65 (70H, br m, H5), 1.40–2.19 (140H, br m, H4), 1.10–1.30 (9H, m, H1, H3)
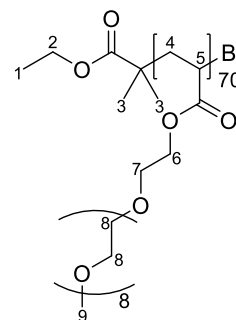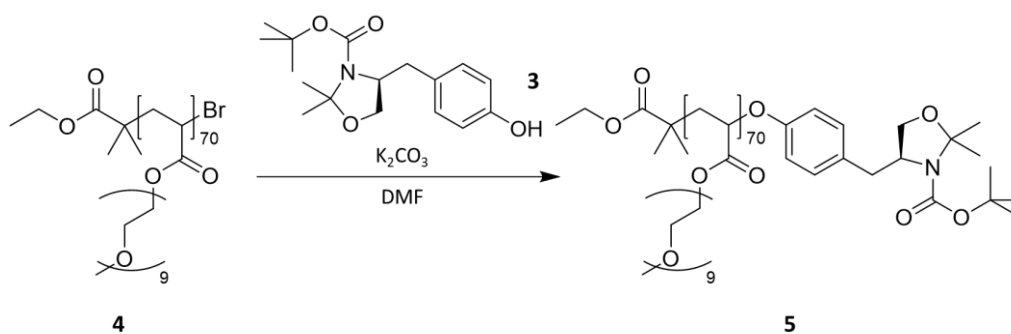

Polymers **8a–8g**

¹H NMR δ_H (400 MHz, CD₃OD): 4.01–4.44 (br m, H15), 3.69–3.78 (br m, H16), 3.50–3.69 (br m, H17), 3.35–3.39 (br, H18), 2.18–2.65 (br m, H14), 1.33–2.18 (br m, H13), 1.27–1.32 (m, H12)
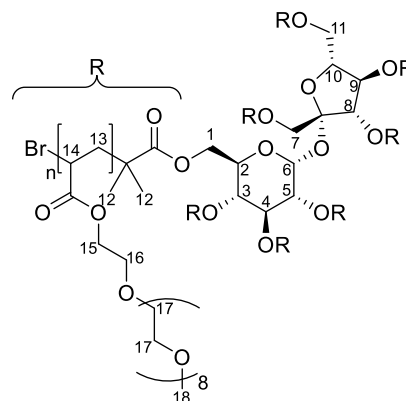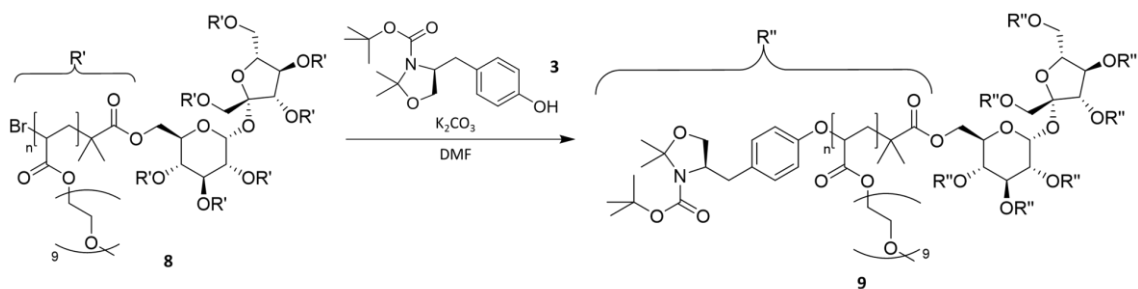

3.5 End group conversions

End group conversions were performed using methods used by previous students.[69,71] Identical methods were used for both the linear and the star polymers.

## 3.5.1 End group linker attachments

Product **3** and K$_2$CO$_3$ were dissolved in DMF. The reaction mixture was heated at 50 °C for 3 hours. Product **4/8** was added to the solution and the reaction mixture was stirred at room temperature for 48 hours. The polymer was precipitated by the dropwise addition of the reaction mixture into cold diethyl ether (10 mL). Polymer was dissolved in deionised water after centrifugation and supernatant decantation. The polymer was purified by dialysis against deionised water. Azeotropic solvent removal with toluene *in vacuo* afforded the product polymers **5**, **9a**, **9f**, and **9g** as light brown oils.

| polymer	product **4/8**	product **3**	K$_2$CO$_3$	DMF	yield
5	m = 50 mg	m = 4.5 mg	m = 0.41 mg	V = 1 mL	m = 20.6 mg
	1 eq	10 eq	2 eq		39 %
5	m = 200 mg	m = 18.1 mg	m = 1.6 mg	V = 2 mL	m = 127.5 mg
	1 eq	10 eq	2 eq		63 %
9a	m = 150 mg	m = 2.2 mg	m = 2.0 mg	V = 1 mL	m = 32.8 mg
	1 eq	10 eq per arm	20 eq per arm		22 %
9f	m = 150 mg	m = 0.53 mg	m = 0.48 mg	V = 1 mL	m = 46.6 mg
	1 eq	10 eq per arm	20 eq per arm		30 %
9g	m = 90 mg	m = 0.40 mg	m = 0.36 mg	v = 1 mL	m = 38.6 mg
	1 eq	10 eq per arm	20 eq per arm		43 %

Polymer **5**

1H NMR δ$_H$ (400 MHz, CD$_3$OD): 7.15 (2H, m, H11), 6.86 (2H, m, H10), 4.13–4.38 (140H, br m, H6), 4.08–4.12 (2H, m, H2), 3.69–3.74 (140H, br m, H7), 3.49–3.69 (2240H, br m, H8), 3.33–3.41 (210H, br, H9), 2.19–2.65 (70H, br m, H5), 1.40–2.19 (140H, br m, H4), 1.10–1.37 (24H, m, H1, H3, H15, H16)
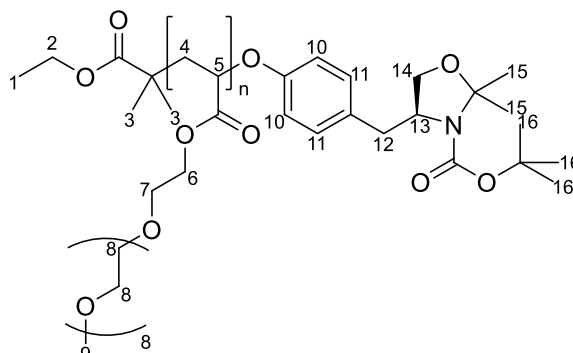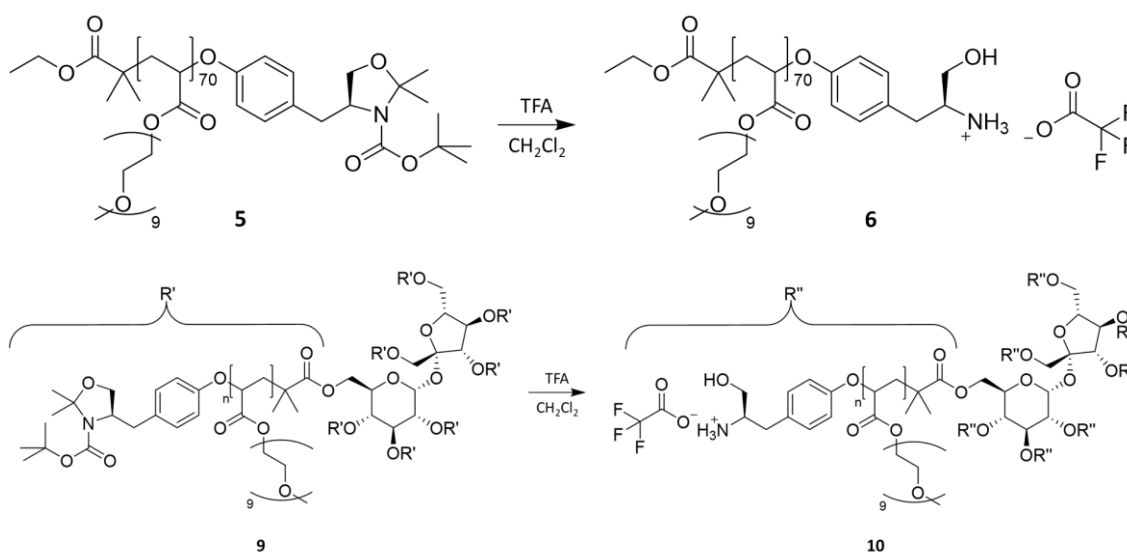
Polymer **9a**

¹H NMR δ_H (400 MHz, CD₃OD): 4.03–4.50 (br m, H15), 3.71–3.81 (br m, H16), 3.52–3.71 (br m, H17), 3.35–3.44 (br, H18), 2.25–2.65 (br m, H14), 1.40–2.10 (br m, H13), 1.28–1.39 (m, H12, H24, H25)
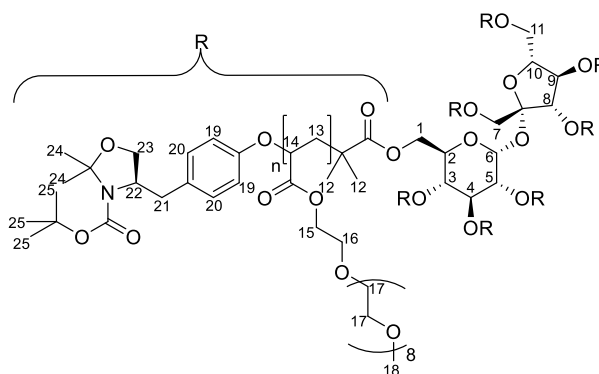
Polymers **9f** and **9g**

¹H NMR δ_H (400 MHz, CDCl₃): 3.93–4.44 (br m, H15), 3.66–3.72 (br m, H16), 3.52–3.66 (br m, H17), 3.37–3.42 (br, H18), 2.13–2.51 (br m, H14), 1.23–2.13 (br m, H13), 1.16–1.45 (m, H12, H24, H25)

3.5.2 Deprotections

Product **5/9** was dissolved in anhydrous dichloromethane. The solution was cooled to 0 °C. Trifluoroacetic acid was added dropwise to the solution. The reaction mixture was stirred at room temperature for 1 h. The solvent and any other volatiles were removed *in vacuo*. The crude product was dissolved in deionised water and purified by dialysis against deionised water. Azeotropic solvent removal with toluene *in vacuo* afforded the products **6**, **10a**, **10f**, and **10g** as light brown oils.

polymer	product 5/9	CH$_2$Cl$_2$	TFA	yield
6	m = 10 mg / 1 eq	V = 0.5 mL	V = 0.5 mL	m = 10.1 mg / 98 %
6	m = 127.5 mg / 1 eq	V = 1 mL	V = 1 mL	m = 102.5 mg / 81 %
10a	m = 32.1 mg / 1 eq	V = 0.5 mL	V = 0.5 mL	m = 21.3 mg / 66 %
10f	m = 46.0 mg / 1 eq	V = 1 mL	V = 1 mL	m = 30.3 mg / 66 %
10g	m = 37.6 mg / 1 eq	V = 1 mL	V = 1 mL	m = 34.4 mg / 92 %

Polymer **6**

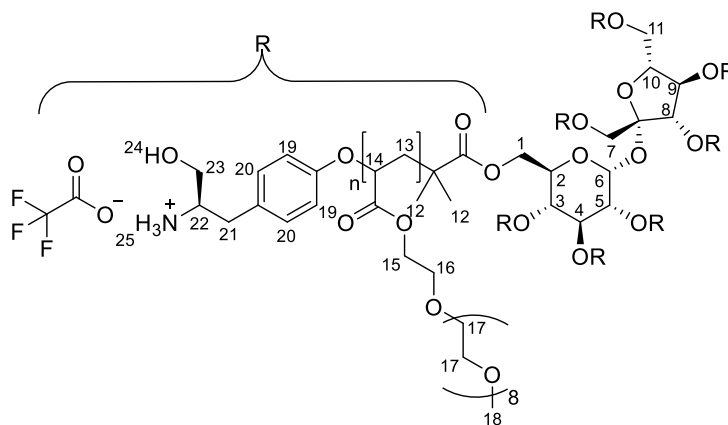**^{1}H NMR** δ_H (400 MHz, CD$_3$OD): 7.15 (2H, m, H11), 6.86 (2H, m, H10), 4.14–4.38 (140H, br m, H6), 4.11–4.14 (3H, m, H2, H13), 3.71–3.81 (140H, br m, H7), 3.52–3.71 (2240H, br m, H8), 3.36–3.42 (210H, br, H9), 2.35–2.60 (70H, br m, H5), 1.41–2.09 (140H, br m, H4), 1.13–1.40 (9H, m, H1, H3)
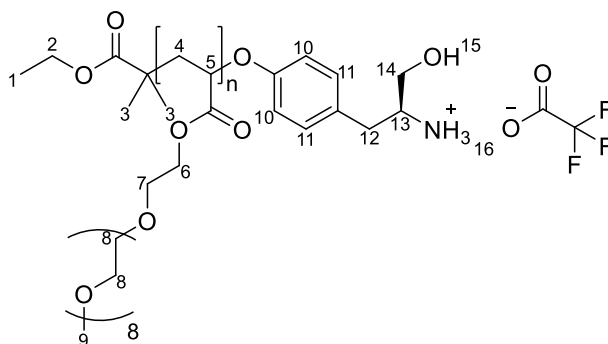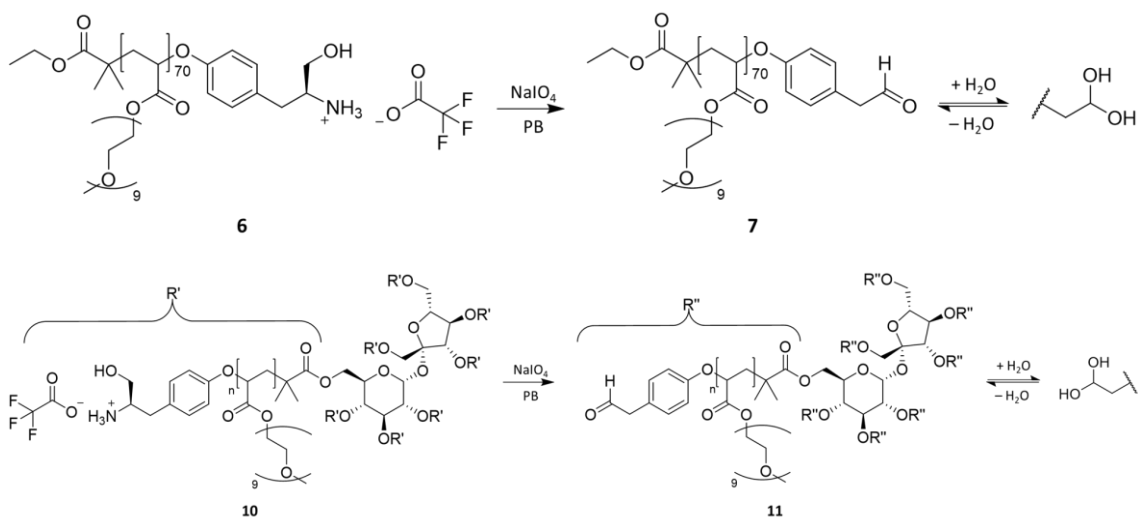
Polymer **10a**

^{1}H NMR δ_H (400 MHz, DMSO): 4.00–4.42 (br m, H15), 3.62–3.72 (br m, H16), 3.46–3.62 (br m, H17), 3.27–3.33 (br, H18), 2.19–2.47 (br m, H14), 1.02–1.99 (br m, H13), 0.85–0.97 (m, H12)

Polymers **10f** and **10g**

^{1}H NMR δ_H (400 MHz, CDCl$_3$): 4.01–4.40 (br m, H15), 3.52–3.80 (br m, H16, H17), 3.35–3.43 (br, H18), 2.14–2.50 (br m, H14), 1.34–1.99 (br m, H13), 1.19–1.34 (m, H12)
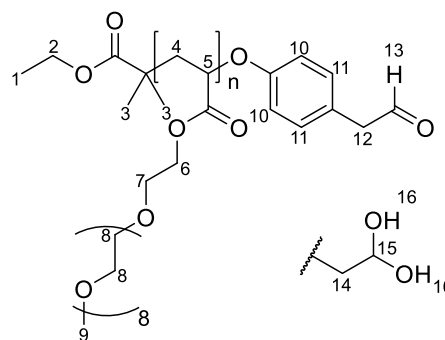
3.5.3 Oxidations

First, a phosphate buffer (100 mM, pH 7.0) was made. Na_2HPO_4 (38 mM) and KH_2PO_4 (62 nM) were dissolved in deionised water and pH was adjusted with aqueous NaOH solution (5 M). Product **6/10** and $NaIO_4$ were dissolved in this phosphate buffer solution. The reaction mixture was stirred at room temperature in the dark for 1 h. The polymer was purified by dialysis against deionised water. Azeotropic solvent removal with toluene *in vacuo* afforded the products **7**, **11a**, **11f**, and **11g** as light brown oils.

| polymer	product **6/10**	$NaIO_4$	phosphate buffer	yield
7	m = 10.1 mg	m = 1.1 mg	V = 1 mL	m = 8.6 mg
	1 eq	2 eq		86 %
7	m = 102.5 mg	m = 10.3 mg	V = 2 mL	m = 93.6 mg
	1 eq	2 eq		92 %
11a	m = 21.3 mg	m = 0.044 mg	V = 1.5 mL	m = 16.5 mg
	1 eq	2 eq per arm		78 %
11f	m = 28.0 mg	m = 0.014 mg	V = 1.5 mL	m = 20.7 mg
	1 eq	2 eq per arm		74 %
11g	m = 33.1 mg	m = 0.012 mg	V = 1.5 mL	m = 31.8 mg
	1 eq	2 eq per arm		96 %

Polymer **7**

^{1}**H NMR** δ_H (400 MHz, CDCl$_3$): 9.82 (0.3H, s, H13), 3.96–4.23 (140H, br m, H6), 3.43–3.70 (2380H, br m, H7, H8), 3.25–3.35 (210H, br, H9), 2.03–2.44 (70H, br m, H5), 1.27–2.03 (140H, br m, H4), 1.02–1.22 (9H, m, H1, H3)
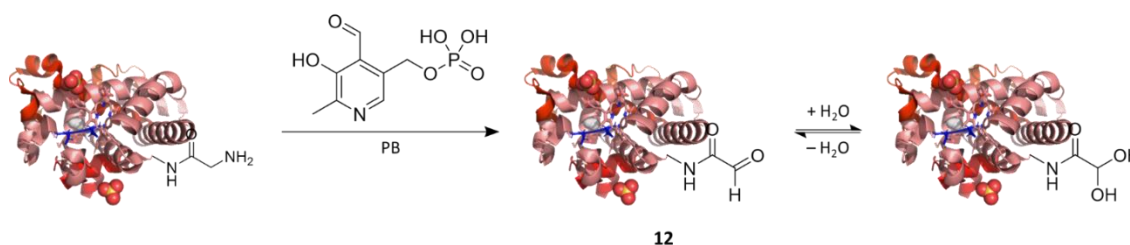
Polymers **11a**, **11f**, and **11g**

^{1}**H NMR** δ_H (400 MHz, CDCl$_3$): 3.88–4.37 (br m, H15), 3.43–3.72 (br m, H16, H17), 3.28–3.34 (br, H18), 2.07–2.40 (br m, H14), 0.92–2.07 (br m, H13)
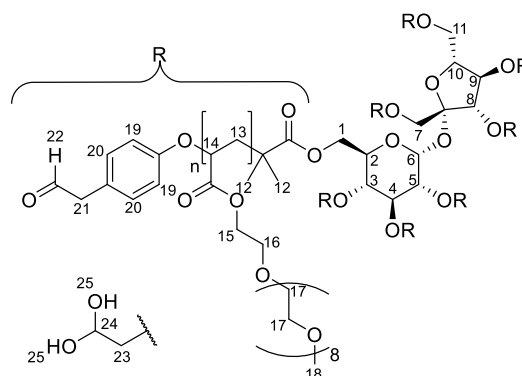
3.6 Myoglobin oxidation to glyoxyl-myoglobin

Myoglobin was oxidised using a method from the literature.[73] First, a phosphate buffer (25 mM, pH 6.5) was made. Na$_2$HPO$_4$ (4 mM) and KH$_2$PO$_4$ (21 mM) were dissolved in deionised water and pH was adjusted with aqueous NaOH solution (5 M). Equine heart myoglobin (0.010 g, 0.59 µmol, 1 eq) and pyridoxal-5-phosphate (0.0364 g, 0.15 mmol, 250 eq) were dissolved in the phosphate buffer (10 mL). The reaction mixture was briefly agitated and then stirred at 37 °C for 24 hours. Next, another phosphate buffer (25 mM, pH 7.5) was made. Na$_2$HPO$_4$ (17 mM) and KH$_2$PO$_4$ (8 mM) were dissolved in deionised water and pH was adjusted with aqueous NaOH solution (5 M). The product was purified by dialysis at 5 °C against this latter phosphate buffer. Product **12** was obtained in a

phosphate buffer solution (0.014 mM, ≈18 mL, ≈4.2 mg, 41 %). **ESI-MS**: found 16950 and 16969, calculated 16950 (for aldehyde form) and 16968 (for hydrate form).

3.7 OPAL reactions
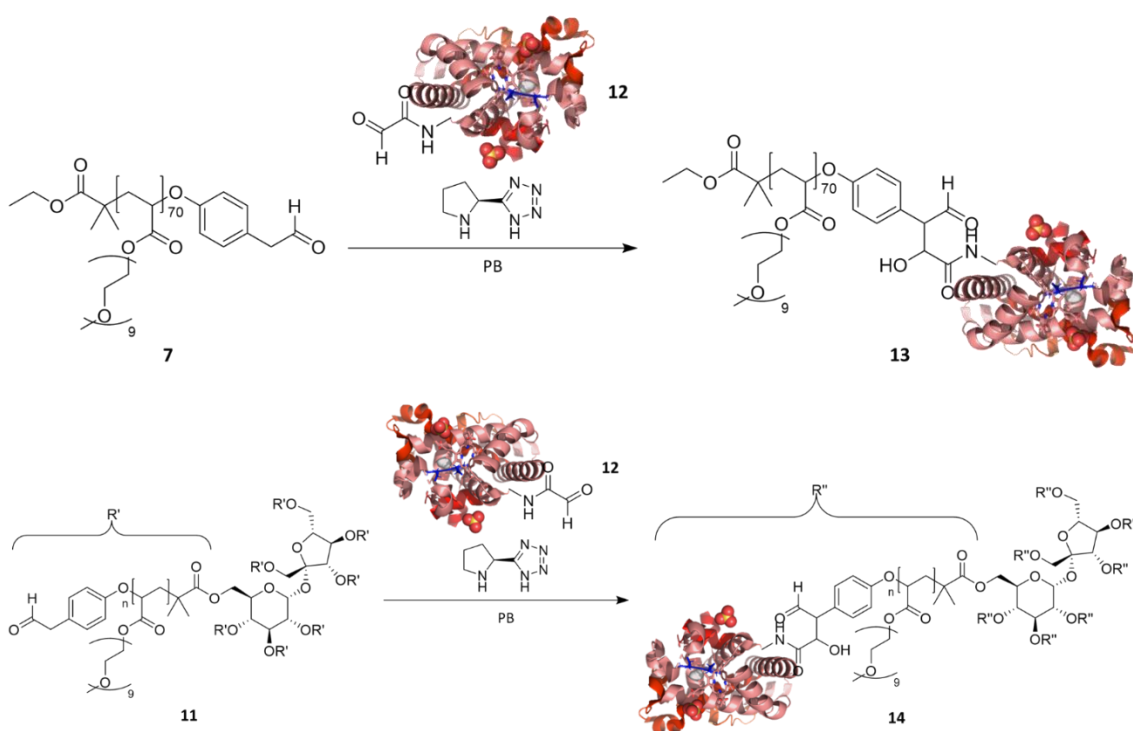
A method from the literature was used for OPAL reactions.[68] Proline tetrazole and product **7/11** were dissolved in a phosphate buffer solution (25 mM, pH 7.5) that contains glyoxyl-myoglobin (**12**). The reaction mixture was mixed by pipetting and without further agitation was then heated at 37 °C for 24 hours.

conjugate	product 7/11	product 12 in phosphate buffer	proline tetrazole
13	m = 4.01 mg	m = 1.00 mg	m = 2.05 mg
		V = 4.24 mL	
	2 eq	1 eq	250 eq
13	m = 2.00 mg	m = 1.99 mg	m = 2.04 mg
		V = 8.45 mL	
	1 eq	2 eq	250 eq
13	m = 2.01 mg	m = 1.00 mg	m = 2.05 mg
		V = 4.24 mL	
	1 eq	1 eq	250 eq
13	m = 20.1 mg	m = 1.00 mg	m = 2.05 mg
		V = 3.20 mL	
	10 eq	1 eq	250 eq
13	m = 71.6 mg	m = 1.00 mg	m = 2.05 mg
		V = 3.20 mL	
	35 eq	1 eq	250 eq
14a	m = 5.85 mg	m = 0.96 mg	m = 3.93 mg
		V = 3.06 mL	
	1 eq	2 eq per arm	250 eq per arm
14f	m = 4.95 mg	m = 0.78 mg	m = 0.80 mg
		V = 2.488 mL	
	1 eq	8 eq per arm	250 eq per arm
14g	m = 7.7 mg	m = 0.90 mg	m = 0.92 mg
		V = 2.874 mL	
	1 eq	8 eq per arm	250 eq per arm

References

1. Antibiotic resistance. https://www.who.int/news-room/fact-sheets/detail/antibiotic-resistance.

2. Antimicrobial resistance. https://www.who.int/news-room/fact-sheets/detail/antimicrobial-resistance.

3. Donaldson, D. M., Roberts, R. R., Larsen, H. S. & Tew, J. G. *Infect. Immun.* **10**, 657–666 (1974).

4. Patterson-Delafield, J., Martinez, R. J. & Lehrer, R. I. *Infect. Immun.* **30**, 180–192 (1980).

5. Rest, R. F., Cooney, M. H. & Spitznagel, J. K. S *Infect. Immun.* **16**, 145–151 (1977).

6. Neu, H. C. *Rev. Infect. Dis.* **7**, S778–S782 (1985).

7. Global Antimicrobial Resistance and Use Surveillance System (GLASS) Report: 2021. https://www.who.int/publications/i/item/9789240027336.

8. Zahedi, A., Hossein, B. & Kafil, S. *Curr. Med. Res. Opin.* **31**, 707–721 (2015).

9. 2020 antibacterial agents in clinical and preclinical development: an overview and analysis. https://www.who.int/publications/i/item/9789240021303.

10. Plackett, B. *Nature* **586**, S50–S52 (2020).

11. Towse, A. *et al. Health Policy (New. York).* **121**, 1025–1030 (2017).

12. Sharma, P. & Towse, A. *SSRN Electron. J.* (2010) doi:10.2139/SSRN.2640028.

13. Theuretzbacher, U. *Clin. Microbiol. Infect.* **23**, 713–717 (2017).

14. Gorter, E. & Grendel, F. *J. Exp. Med.* **41**, 439–443 (1925).

15. Saier, M. H. Bacterial and archaeal cell membranes. in *Encyclopedia of Microbiology* 333–347 (Elsevier, 2019).

16. Cappuccino, J. G. & Sherman, N. Bacterial staining. in *Microbiology : A Laboratory Manuall* 477 (Benjamin/Cummings, 1999).

17. Richmond, M. H. & Curtis, N. A. C. *Ann. N. Y. Acad. Sci.* **235**, 553–568 (1974).

18. Plésiat, P. & Nikaido, H. *Mol. Microbiol.* **6**, 1323–1333 (1992).

19. Vaara, M., Plachy, W. Z. & Nikaido, H. *Biochim. Biophys. Acta* **1024**, 152–158 (1990).

20. Duerr, C. U. *et al. PLoS Pathog.* **5**, 1000567/1-1000567/13 (2009).

21. Murray, G. L., Attridge, S. R. & Morona, R. *J. Bacteriol.* **188**, 2735–2739 (2006).

22. Saldías, M. S., Ortega, X. & Valvano, M. A. *J. Med. Microbiol.* **58**, 1542–1548 (2009).

23. Osborn, M. J., Gander, J. E., Parisi, E. & Carson, J. *J. Biol. Chem.* **247**, 3962–3972 (1972).

24. Braun, V. *FEMS Microbiol. Rev.* **16**, 295–307 (1995).

25. Nakae, T. *Biochem. Biophys. Res. Commun.* **71**, 877–884 (1976).

26. Koebnik, R., Locher, K. P. & Van Gelder, P. *Mol. Microbiol.* **37**, 239–253 (2000).

27. Koebnik, R., Locher, K. P. & Van Gelder, P. *Mol. Microbiol.* **37**, 239–253 (2000).

28. De Mot, R. & Vanderleyden, J. *Mol. Microbiol.* **12**, 333–334 (1994).

29. Koebnik, R. *Mol. Microbiol.* **16**, 1269–1270 (1995).

30. Heffernan, E. J. *et al.* S *Infect. Immun.* **62**, 5183–5186 (1994).

31. Luckey, M. & Nikaido, H. *Proc. Natl. Acad. Sci. U. S. A.* **77**, 167–171 (1980).

32. Scandella, C. J. & Kornberg, A. *Biochemistry* **10**, 4447–4456 (1971).

33. Bassford, P. J., Bradbeer, C., Kadner, R. J. & Schnaitman, C. A. *J. Bacteriol.* **128**, 242–247 (1976).

34. Frost, G. E. & Rosenberg, H. *J. Bacteriol.* **124**, 704–712 (1975).

35. Dorit, R. L. *et al. The Bacteriocins: Current Knowledge and Future Prospects.* (2016).

36. Davies, J. K. & Reeves, P. *J. Bacteriol.* **123**, 102–117 (1975).

37. Davies, J. K. & Reeves, P. *J. Bacteriol.* **123**, 96–101 (1975).

38. Kleanthous, C. *Nat. Rev. Microbiol.* **8**, 843–848 (2010).

39. Ames, G. F. L. & Nikaido, K. *Biochemistry* **15**, 616–623 (1976).

40. Rassam, P. *et al. Nature* **523**, 333–336 (2015).

41. Jenkins, A. D., Stepto, R. F. T., Kratochvíl, P. & Suter, U. W. *Pure Appl. Chem.* **68**, 2287–2311 (1996).

42. Chremos, A. & Douglas, J. F. *J. Chem. Phys.* **143**, 111104/1-111104/5 (2015).

43. Chremos, A., Glynos, E. & Green, P. F. *J. Chem. Phys.* **142**, 044901/1-044901/9 (2015).

44. Chremos, A., Jeong, C. & Douglas, J. F. *Soft Matter* **13**, 5778–5784 (2017).

45. Wu, W., Wang, W. & Li, J. *Prog. Polym. Sci.* **46**, 55–85 (2015).

46. Rhodes, Robert, B. Star polymer viscosity index improver for oil compositions - Google Patents - WO1999042542A1. (1999).

47. Warfel, D. R. & Milkovich, R. Thermoplastic star-block elastomers - Google Patents

- EP0025353A1. (1981).

48. Hadjichristidis, N. *et al.* Polymers with Star-Related Structures: Synthesis, Properties, and Applications. in *Polymer Science: A Comprehensive Reference, 10 Volume Set* vol. 6 29–111 (Elsevier, 2012).

49. Okay, O. & Funke, W. *Makromol. Chem., Rapid Commun* **11**, 583–587 (1990).

50. Kanaoka, S., Sawamoto, M. & Higashimura, T. *Macromolecules* **24**, 2309–2313 (1991).

51. Miura, Y. & Yoshida, Y. *Polym. J.* **34**, 748–754 (2002).

52. Pitto, V., Voit, B. I., Loontjens, T. J. A. & Van Benthem, R. A. T. M. *Macromol. Chem. Phys.* **205**, 2346–2355 (2004).

53. Darcos, V. *et al. Chem. Commun.* 2110–2111 (2004) doi:10.1039/B407508K.

54. Aksakal, R., Resmini, M. & Becer, C. R. *Polym. Chem.* **7**, 171–175 (2016).

55. Maglio, G., Nese, G., Nuzzo, M. & Palumbo, R. *Macromol. Rapid Commun.* **25**, 1139–1144 (2004).

56. Zhu, Z., Rider, J., Yang, C. Y., Gilmartin, E. & Wnek, G. E. S *Macromolecules* **25**, 7330–7333 (1992).

57. Bazan, G. C. & Schrock, R. R. S*Macromolecules* **24**, 817–823 (1991).

58. Fraser, C. L., Smith, A. P. & Wu, X. *J. Am. Chem. Soc.* **122**, 9026–9027 (2000).

59. Gozgen, A. *et al. J. Polym. Sci. Part A Polym. Chem.* **47**, 497–504 (2009).

60. Szwarc, M., Levy, M. & Milkovich, R. *J. Am. Chem. Soc.* **78**, 2656–2657 (1956).

61. Percec, V. *et al. J. Am. Chem. Soc.* **128**, 14156–14165 (2006).

62. Percec, V. *et al. J. Am. Chem. Soc.* **124**, 4940–4941 (2002).

63. Cardinale, A., Isse, A. A., Gennaro, A., Robert, M. & Savéant, J. M. *J. Am. Chem. Soc.* **124**, 13533–13539 (2002).

64. Krall, N., Da Cruz, F. P., Boutureira, O. & Bernardes, G. J. L. *Nat. Chem.* **8**, 103–113 (2015).

65. Van Kasteren, S. I. *et al. Nature* **446**, 1105–1109 (2007).

66. Changa, P. V. *et al. Proc. Natl. Acad. Sci. U. S. A.* **107**, 1821–1826 (2010).

67. Macdonald, J. I., Munch, H. K., Moore, T. & Francis, M. B. *Nat. Chem. Biol.* **11**, 326–331 (2015).

68. Spears, R. J. *et al. Chem. Sci.* **9**, 5585–5593 (2018).

69. Tomkins, J. R. Star Polymer-protein Conjugates to Study Movement of Proteins in Bacterial Cell Membranes. (Durham University, 2020).

70. Stenzel-Rosenbaum, M. H., Davis, T. P., Chen, V. & Fane, A. G. *Macromolecules* **34**, 5433–5438 (2001).

71. Roberts, I. Star Polymer-Protein Conjugates to Study OMP Movement in E. coli. (Durham University, 2021).

72. Lishchynskyi, O. *et al. Materials (Basel).* **14**, 1417–1438 (2021).

73. Gilmore, J. M. *et al. Angew. Chemie Int. Ed.* **45**, 5307–5311 (2006).

74. Castro-Forero, A., Jiménez, D., López-Garriga, J. & Torres-Lugo, M. *J. Appl. Polym. Sci.* **107**, 881–890 (2008).

75. Goldschmidt, B. S. *et al. Biomed. Opt. Express* **4**, 2463–2477 (2013).

76. Chen, J., Nie, J., Huang, Y., Chen, Z. & Yang, G. *J. Chem. Res.* **130**, 696–697 (2019).